

Invited Review

The Potential of White Dwarf Cosmochronology¹

G. FONTAINE, P. BRASSARD, AND P. BERGERON

Département de Physique, Université de Montréal, C.P. 6128, Succ. Centre-Ville, Montréal, QC H3C 3J7, Canada;
fontaine@astro.umontreal.ca, brassard@astro.umontreal.ca, bergeron@astro.umontreal.ca

Received 2000 December 8; accepted 2000 December 8

ABSTRACT. In the light of recent significant progress on both the observational and theoretical fronts, we review the status of white dwarf stars as cosmochronometers. These objects represent the end products of stellar evolution for the vast majority of stars and, as such, can be used to constrain the ages of various populations of evolved stars in the Galaxy. For example, the oldest white dwarfs in the solar neighborhood (the remnants of the very first generation of intermediate-mass stars in the Galactic disk) are still visible and can be used, in conjunction with cooling theory, to estimate the age of the disk. More recent observations suggest the tantalizing possibility that a population of very old white dwarfs inhabits the Galactic halo. Such a population may contribute significantly to baryonic “dark” matter in the Milky Way and may be used to obtain an independent estimate of the age of the halo. In addition, white dwarf cosmochronology is likely to play a very significant role in the coming era of giant 8–10 m telescopes when faint white dwarf populations should be routinely discovered and studied in open and globular clusters.

1. INTRODUCTION

White dwarf stars represent the endpoint of the evolution of stars with initial masses ranging from about 0.07 to about $8 M_{\odot}$. This large range encompasses the vast majority of stars formed in the Galaxy, and thus white dwarf stars represent the most common endpoint of stellar evolution. It is believed that over 97% of the stars in the Galaxy will eventually end up as white dwarfs. The defining characteristic of these objects is the fact that their mass is typically of the order of half that of the Sun, while their size is more akin to that of a planet. Their compact nature gives rise to large average densities, large surface gravities, and low luminosities.

The usefulness of white dwarf stars as cosmochronometers was recognized more than 40 years ago by Schmidt (1959), but it is only in the last decade or so that the potential of white dwarf cosmochronology reached a practical level of application. This is because the intrinsic faintness of the coolest, oldest white dwarfs in a given population has made them difficult to observe. In addition, realistic models of such cool, evolved white dwarfs have also been difficult to compute because of uncertainties in the input constitutive physics in this extreme regime of very low effective temperatures. Nevertheless, progress on both fronts has been made, and Winget et al. (1987) were the first to demonstrate that the deficit of very low luminosity white dwarfs in the solar neighborhood discovered by Liebert, Dahn, & Monet (1988) could be most naturally

explained in terms of the finite age of the white dwarf population in the Galactic disk. Their method has been followed by several other groups since, and it is still being refined currently for improved estimates of the age of the disk. These latter efforts incorporate the results of more recent observations which have confirmed the reality of the downturn of the local white dwarf luminosity function at low luminosities.

The quantitative study of white dwarf stars has traditionally relied on photometric and spectroscopic observations of various samples of nearby objects. It should be pointed out, in this context, that spectroscopy, as a practical tool, is limited to such local samples. Again, because of the intrinsic faintness of the most common white dwarfs, observations of these objects tend to be restricted to small distances. For example, the bulk of the *spectroscopic* sample of ~ 2200 white dwarfs available today resides well within ~ 500 pc from the Sun. As a consequence, the vast majority of these stars are representative of only that part of the Galaxy, the local disk, which contains the solar neighborhood.

Other observational techniques have revealed the presence of white dwarf populations located well beyond our own neighborhood, however. For instance, the first glimpses of faint white dwarfs in distant open and globular clusters have been obtained through color photometry, typically two-band photometry, on 4 m class telescopes. The advent of the *Hubble Space Telescope* and, more recently, of the giant 8–10 m ground-based telescopes now allow astronomers to study more quantitatively these faint populations through multiband photometry. In addition, microlensing experiments and direct imaging techniques have led recently to the suggestion of the existence of an ancient

¹ Based, in part, on the C. S. Beals Lecture presented by G. Fontaine at the Annual General Meeting of the Canadian Astronomical Society held in Vancouver (2000 May).

white dwarf population in the Galactic halo. Such cool, old white dwarfs could contribute quite significantly to baryonic “dark” matter in our galaxy. We point out here that Liebert, Dahn, & Monet (1989) already suggested the possible existence of such a halo population some time ago on the basis of the detection of *local* white dwarfs showing unusually large space velocities and best interpreted as interlopers from the halo.

These exciting developments have led to a renewed interest in white dwarf cooling calculations and model atmosphere calculations using upgraded constitutive physics and extending into the regime of very low effective temperatures as appropriate for the cool, evolved white dwarfs that populate the disk, the halo, and the Galactic clusters. Along with several groups in the world, we are currently building these “next-generation” white dwarf models. Using representative examples, we review these current efforts in the light of the most recent observations available. Our goal here is not so much to provide the reader with “definitive answers” but, rather, to demonstrate the potential of white dwarf cosmochronology.

We begin, in the next section, by reminding the reader of the basic properties of white dwarf stars. We next discuss the essential characteristics of typical models of evolving white dwarfs obtained through modern, detailed calculations. We next illustrate how the ages of various white dwarf populations can be estimated (1) locally, (2) in open and globular clusters, and (3) in the halo. We finally discuss the current limitations of white dwarf cosmochronology, and we conclude with a brief summary.

2. BASIC PROPERTIES OF WHITE DWARF STARS

Several properties of white dwarf stars can be determined fairly directly from observations. Analyses of their energy distribution, as well as of their optical and ultraviolet spectra, fix their effective temperature; they range from $\sim 150,000$ K for the hottest stars to T_{eff} near 4000 K for the coolest degenerate dwarfs (but see below). Spectroscopic analyses also yield the surface gravity, $\log g$, since the strength and width of spectral features are sensitive to the density of particles in the atmosphere, which is controlled by the surface gravity. For the cooler white dwarfs, however, the spectral features have all but vanished, and spectroscopic estimates of $\log g$ are no longer available. In such cases, parallax measurements can be used to determine the radius and the mass (through a mass-radius relation) and, hence, the surface gravity. The average surface gravity of white dwarf stars is $\log g \sim 8$ (cm s^{-2}), compared to $\log g \sim 4.4$ for the Sun. The luminosity range encompassed by white dwarfs exceeds 7 orders of magnitude and reflects the large range of observed effective temperatures ($L \propto T_{\text{eff}}^4$); the faintest known white dwarfs have $L \sim 10^{-4.7} L_{\odot}$, while the rare intrinsically brighter ones, just entering the cooling sequence, reach $L \sim 10^2\text{--}10^3 L_{\odot}$. The average visual magnitude of the spectroscopically confirmed (local) white dwarfs is $V \sim 15.5$.

Traditionally, white dwarfs have been culled from samples of

objects showing significant proper motion and thus located relatively nearby the Sun. A selection criterion based on color then allows the distinction to be made between true white dwarfs and nearby main-sequence stars, and their degenerate nature is then confirmed through spectroscopic observations. More recently, large numbers of hot white dwarfs have been detected in colorimetric searches. Selected fields are typically photographed through both *U* and *B* filters. A comparison of both images for a given object allows the selection of blue or very blue objects, whose nature can be confirmed through spectroscopic means. Surveys of this kind, carried out both at high Galactic latitude and in the plane of the Galaxy, have yielded substantial numbers of new hot white dwarfs, selected only on the basis of their colors without regard for their proper motion.

The existence of homogeneous samples containing substantial numbers of white dwarfs allows analyses of the statistical properties of these objects. For example, it is now well established that the distribution of white dwarfs in our neighborhood is consistent with that of an old disk population, with an estimated scale height of 250–300 pc. Their space density is of the order of 0.005 pc^{-3} for $M_{\text{bol}} < 15$, and their birthrate is of the order of $(1.5\text{--}2.3) \times 10^{-12} \text{ pc}^{-3} \text{ yr}^{-1}$ when allowance is made for the contribution of unseen white dwarfs in binary systems.

It is generally believed that the immediate progenitors of most white dwarfs are nuclei of planetary nebulae, themselves the products of intermediate- and low-mass main-sequence evolution. As mentioned above, stars that begin their lives with masses less than about $8 M_{\odot}$, that is, the vast majority of them, are expected to become white dwarfs. Among those which already have had the time to become white dwarfs since the formation of the Galaxy, a majority have burned hydrogen and helium in their interiors. Consequently, most of the mass of a typical white dwarf is contained in a core made of the products of helium burning, mostly carbon and oxygen. The exact proportions of C and O are unknown because of uncertainties in the nuclear rates of helium burning.

The observed mass distribution of isolated white dwarfs is sharply peaked, and the mean mass is $0.59 M_{\odot}$. Even though low-amplitude tails (suspected to be the products of binary evolution) extend at both ends of the mass spectrum, from ~ 0.3 to $\sim 1.2 M_{\odot}$, the bulk of the field white dwarfs have masses that cluster around the mean value with a small dispersion $\sigma \approx 0.13 M_{\odot}$. This relatively narrow mass distribution is a remarkable property of this category of stars. Apparently, the process of mass loss in white dwarf progenitors, which may have a wide range of initial masses, is regulated by mechanisms that are tuned finely enough to leave remnants with similar masses consistently. Also, the empirical evidence suggests that small amounts of helium and hydrogen are left over after the mass-loss phases have subsided. Taking into account previous thermonuclear history and the efficiency of gravitational settling, the expected structure of a typical white dwarf is that of a compositionally stratified object with a mass of $\sim 0.6 M_{\odot}$.

consisting of a carbon-oxygen core surrounded by a thin, helium-rich envelope itself surrounded by a hydrogen-rich layer. Such an object has an average density of $\sim 10^6 \text{ g cm}^{-3}$, a millionfold that of a normal star such as the Sun. The respective thicknesses of the hydrogen and helium outer layers are not known a priori and must depend on the details of pre-white dwarf evolution. On theoretical grounds, however, it is expected that the maximum amount of helium that can survive nuclear burning in the hot planetary nebula phase is only about 10^{-2} of the total mass of the star and that the maximum fractional mass of hydrogen is about 10^{-4} . Although these outer layers are very thin, they are extremely opaque to radiation and regulate the energy outflow from the star. They consequently play an essential role in the evolution of a white dwarf. The question of the exact masses of the hydrogen and helium layers present in white dwarfs constitutes a topic of intense research interest in the field.

The large opacity of the outer layers of a white dwarf implies that radiation escaping from the star originates from the outermost region—the atmosphere—which contains, typically, less than 10^{-14} of the total mass of the star. Spectroscopic and photometric observations can only probe these outer regions, which are usually dominated by hydrogen. Thus, a majority of white dwarfs are referred to as hydrogen-atmosphere objects (also termed DA stars). It turns out, however, that about 25% of the known white dwarfs do not possess such a hydrogen layer. These are called helium-atmosphere white dwarfs (or non-DA stars) with, again, the understanding that the underlying carbon-oxygen core must contain essentially all of the mass, even though it is not directly observable.

There is strong observational evidence that spectral evolution takes place among white dwarfs, that is, some of the hydrogen-atmosphere stars become helium-atmosphere objects, and vice versa, during various evolutionary phases. Indeed, the ratio of DA to non-DA white dwarfs changes as a function of effective temperature along the cooling sequence. In particular, the cases for the existence of a so-called DB gap—an interval of effective temperature from 45,000 K to about 30,000 K in which *no* helium-atmosphere object has been found—and of a cooler and narrower non-DA gap between ~ 6000 K and ~ 5000 K are well documented. Completely convincing explanations for these phenomena (especially in the case of the cooler gap) have not been worked out yet, but the very existence of “holes” in the distribution of helium-atmosphere objects as a function of effective temperature is a strong empirical proof that, at least, some of the white dwarf stars must change their superficial chemical composition from helium-dominated to hydrogen-dominated and back to helium-rich again as evolution proceeds. It is suspected that a complex interplay between mechanisms such as hydrogen and helium separation (through diffusion) and convective dilution and mixing is responsible for the fact that a white dwarf may show two different “faces” during its lifetime.

As former nuclei of planetary nebulae, most white dwarfs are born in the form of extremely hot, collapsed objects which

can only cool off: Their nuclear energy sources are depleted, and gravitational energy can no longer be tapped efficiently as degenerate electron pressure prevents additional contraction. Because this pressure is independent of the temperature, a white dwarf is condemned to evolve at essentially constant radius. The mechanical structure of such a star is therefore largely specified by the degenerate electrons. In particular, electron degeneracy is directly responsible for the curious relationship between the mass and the radius of a white dwarf: The more massive the star, the smaller its size is. Likewise, relativistic degeneracy is also responsible for the existence of a limiting mass above which a white dwarf cannot exist—the famous Chandrasekhar mass.

Degenerate electrons also possess another property of high relevance for white dwarfs: They are excellent conductors of heat, and thus they thermalize the internal regions of white dwarfs efficiently. We can thus envision a typical white dwarf as consisting of a nearly isothermal core that contains more than 99% of the mass, surrounded by a thin, opaque, insulating, nondegenerate outer envelope. In the range of effective temperatures 16,000–8000 K where the bulk of the known white dwarfs is found, core temperatures vary from $\sim 2 \times 10^7$ K to $\sim 5 \times 10^6$ K. The very large temperature drop between the central regions and the surface takes place mainly in the stellar envelope. In the cooler models, this temperature gradient leads to the formation of superficial convection zones, similar to that found in the Sun. When present, atmospheric convection plays an essential role in the determination of the emergent flux from a white dwarf and, thus, in the interpretation of its spectrum and colors. Convection plays also a key role in the subsequent evolution of a white dwarf by affecting directly the cooling rate. This occurs when the base of the superficial convection zone reaches into the degenerate interior, thus coupling the surface with the core and, thereby, increasing the rate of energy transfer across the outer opaque envelope beyond what is possible through radiative transfer alone. This process, which we refer to as “convective coupling,” constitutes a significant “event” and is of fundamental importance in the evolution of cool white dwarfs.

Largely decoupled from the electrons, the (nondegenerate) ions provide the thermal energy that slowly leaks through the outside, thereby producing the star’s luminosity. Thus, an isolated white dwarf shines at the expense of its thermal reservoir. In this context, the electrons do not contribute significantly to the energy reservoir because degenerate particles, already occupying their states of lowest energy, cannot be cooled. As thermal energy is gradually lost from the star in the form of radiation, the kinetic motions of the ions lose amplitude and become correlated, and the ionic state evolves from a gas to a fluid to a solid. The liquid-to-solid transition in the cooling cores of white dwarfs is a first-order phase transition and, consequently, is accompanied by a concomitant release of latent heat providing an energy of the order of $\sim 1 \text{ kT}$ per ion, a significant amount of energy, able to slow down considerably

the cooling process. Ultimately, however, the reservoir of thermal energy becomes depleted, and the star disappears from sight in the form of a cooled-off, crystallized object known as a black dwarf. Crystallization, along with the associated release of latent heat, is the other significant “event” in the evolution of cool white dwarfs.

In order to use white dwarfs as cosmochronometers, it is necessary to compute their cooling rates. It is here that the intimate relationship between dense-matter physics and the structure and evolution of white dwarfs enters into the picture. Indeed, this rate basically depends on two items: (1) how much thermal energy is stored in the interior of a star and (2) how rapidly this energy is transferred from the hot core to the cold interstellar medium through the thin opaque outer layers. On the first account, one needs a detailed understanding of the thermodynamics of the fluid/solid core to compute the energy contained in the thermal reservoir. On the second account, one needs to solve in detail the energy transfer problem across the star. This requires an accurate description of the thermodynamics, the radiative, and conductive opacities of the gas/fluid envelope. In addition, convective transport must also be handled, and realistic model atmospheres must be used as outer boundary conditions.

To see this better, we recall a well-known equation for the luminosity, L , of a homogeneous star as a function of time t ,

$$L(t) = \int_0^M \left(\epsilon - T \frac{\partial S}{\partial \rho} \bigg|_r \frac{\partial \rho}{\partial t} - C_v \frac{\partial T}{\partial t} \right) dm, \quad (1)$$

where ϵ is the rate of energy production through thermonuclear means minus the rate of energy loss through neutrino cooling processes per gram of stellar material, where the second term in the integral corresponds to the rate of gravitational energy release (per gram), and where the third term corresponds to the rate of thermal energy release (per gram). The integral is carried over the mass of the star, T is the temperature, S is the entropy per gram, ρ is the density, and C_v is the specific heat per gram at constant volume. In a first approximation, if we assume that residual gravitational contraction is negligible in a white dwarf ($\partial \rho / \partial t = 0$), if we assume that the star is strictly isothermal ($T = T_c = \text{constant}$), and if we assume that residual energy sources and sinks are zero ($\epsilon = 0$), then we can transform equation (1) to obtain an estimate of the interval of time, t_{cool} , required for the star to cool from a luminosity L_1 to a lower luminosity L_2 ,

$$t_{\text{cool}} \simeq - \int_0^M C_v dm \times \int_{L_1}^{L_2} \frac{\partial T_c}{\partial L} \frac{dL}{L}. \quad (2)$$

The first integral on the right-hand side of equation (2), the integrated specific heat, is very clearly related to the thermal energy content of the star (item 1 above). Likewise, the second integral involves the relation between the core temperature,

T_c , and the surface luminosity, L , which is given directly by the solution of the heat transfer problem from the core to the surface (item 2 above). We immediately point out, on the basis of equation (2), that C core white dwarfs take generally longer to cool to a given luminosity than O core stars because, in the fully ionized interior, the specific heat per gram of carbon is larger than that of oxygen (there are more ions in a gram of carbon than in a gram of oxygen).

To recover the classic result of Mestel (1952) for t_{cool} , other approximations must be made. As discussed in the superb review paper of Van Horn (1971), those are (1) the neglect of the electronic heat capacity, i.e., $C_v = C_v(\text{ions})$, (2) the use of the perfect gas law for ions, $C_v(\text{ions}) = (3N_0 k)/(2A)$, where N_0 is Avogadro’s number and A is the atomic weight of the core material, (3) the assumption of strict radiative equilibrium in the partially degenerate envelope, and (4) the use of an analytic model (a Kramers’ law) for the radiative opacity in the envelope. With these additional approximations, one finds the following well known trends,

$$t_{\text{cool}}^{\text{Mestel}} \propto A^{-1} \mu^{-2/7} M^{5/7} L^{-5/7}, \quad (3)$$

where μ is the mean molecular weight of the material in the envelope. Equation (3) shows how, within the framework of the Mestel model, the cooling time of a white dwarf is related to its core chemical composition, its envelope chemical composition, its mass, and its luminosity. However, we must point out that while Mestel’s original theory has played an essential role in the historical development of the field, none of the last approximations is justified in the regime of low effective temperatures that is crucial for white dwarf cosmochronology. Consequently, only detailed models are appropriate.

3. DETAILED MODELS OF COOLING WHITE DWARFS

3.1. A Brief Historical Survey

It is not our purpose here to review the rich and extensive literature on white dwarf cooling theory. Instead, we only mention briefly what, in our view, have constituted the major theoretical milestones toward making white dwarf cosmochronology a practical tool. The stage was first set by Van Horn (1971), who delineated very clearly the improvements to be made to the classic Mestel theory of cooling white dwarfs, and the next standards were established by his group at Rochester. Thus, a full evolutionary code, bypassing all the approximations discussed just above, was developed by Lamb (1974; see also Lamb & Van Horn 1975). This code featured the inclusion of the first detailed thermodynamic description of the dense fully ionized fluid/solid core plasma, including the release of latent heat upon crystallization. It also incorporated the envelope code of Fontaine (1973) for the computations of the envelope structures and of the outer boundary conditions. The latter featured the first detailed calculations of the equation of

state in the difficult regime of partially ionized and partially degenerate plasmas (Fontaine, Graboske, & Van Horn 1977), as well as a full description of convective transport (Fontaine & Van Horn 1976). The conductive opacities used were those of Hubbard & Lampe (1969), and the radiative opacities were taken from Cox & Stewart (1970). Lamb & Van Horn (1975) presented the results of a computation for a pure C model with a mass of $1 M_{\odot}$. In the light of the exciting discovery of a downturn in the local white dwarf luminosity function as reported by Liebert et al. (1988), Winget et al. (1987) used the same tools as Lamb & Van Horn (1975) to compute the theoretical luminosity function of local white dwarfs on the basis of pure C models with $M = 0.4, 0.6, 0.8,$ and $1.0 M_{\odot}$. A comparison of the two luminosity functions led them to a preliminary estimate of the age of the Galactic disk. This pioneering effort has been followed by others, incorporating increasingly sophisticated models of cooling white dwarfs and of the relationships with their progenitors.

The importance of Galactic evolution effects in the computation of the theoretical white dwarf luminosity function was emphasized by Iben & Laughlin (1989; see also Yuan 1989), but we note that the point had been foreseen earlier by D’Antona & Mazzitelli (1978) in a somewhat different context. This development was further explored by Wood (1990), who presented a very thorough investigation of the problem in his Ph.D. thesis. Wood used the same evolutionary code as Winget et al. (1987) but considered more realistic compositionally stratified white dwarf models with various core compositions, from pure C to pure O. His computations also included improvements at the level of the constitutive physics with the newer radiative opacities of W. F. Huebner (1980, private communication) and the conductive opacities of Itoh et al. (1983, 1984). His main results were published in Wood (1992). At the time, the general belief favored DA white dwarf structures with “thin” hydrogen layers, so it was expected that these layers would not play an important role in the cooling process. In practice, Wood (1992) idealized the situation by considering only non-DA models, with no hydrogen layer at all. After the pendulum of wisdom swung from the favored “thin” H-layer white dwarf models to “thick” layered models within a few years (see Fontaine & Wesemael 1997 for a discussion of this issue), Wood (1995) presented new calculations appropriate for DA white dwarfs with the maximum possible fractional mass of hydrogen, 10^{-4} . In the process, he incorporated the improved radiative opacities of Rogers & Iglesias (1992) and those of Lenzuni, Chernoff, & Salpeter (1991) at low temperatures. Wood’s calculations cover a wide volume in parameter space and remain, to this day, a standard reference in the field of white dwarf cosmochronology. However, they suffer from some limitations that have been studied by others since. The most severe of those is the built-in use of static envelopes in the evolutionary code which does not allow the crystallization front to propagate into the envelope at low enough luminosities. This forced Wood (1990) to devise an *extrapolation* scheme to es-

timate the cooling times in the regime of very low effective temperatures, which is the regime of interest for white dwarf cosmochronology, particularly for the halo and clusters. The second limitation is related to the use of gray atmospheres as surface boundary conditions. At low enough luminosities, when convective coupling has occurred, nongray effects in the atmosphere become of importance as they shift the location of the superficial convection zone and, thereby, affect the cooling times. Finally, the sedimentation between C and O upon crystallization in models with mixed core compositions has not been included in Wood’s calculations. Sedimentation produces a small but significant delay in the cooling time. For instance, Chabrier et al. (2000) find that the cooling time of a typical $0.6 M_{\odot}$ DA white dwarf to a luminosity $L = 10^{-4.5} L_{\odot}$ is increased by some 14% in presence of C/O sedimentation.

The physics of element sedimentation in the crystallizing cores of white dwarfs, first investigated by Stevenson (1980), has been well articulated in a series of important papers starting with Garcia-Berro et al. (1988) and culminating with Salaris et al. (1997). Galactic evolution models comparable to those used by Wood (1990) were folded in the calculation of the luminosity function of disk white dwarfs (Hernanz et al. 1994). In addition, this approach advertized an improved description of the thermodynamics of the white dwarf interior (Segretain et al. 1994). The main emphasis, however, was put on the phase diagram of a fully ionized binary mixture such as the dense C/O plasma expected in the core of a typical white dwarf. The latest calculations, those of Segretain & Chabrier (1993), indicate that C and O separate upon crystallization according to a spindle-shaped phase diagram. Their result implies that the outward-moving crystallization front in a cooling white dwarf leaves behind a solid region that is O-enriched compared to the original C/O fluid mixture and that the degree of enrichment depends upon the actual composition of the fluid. The extra carbon in the fluid phase is forced upward from a crystallizing shell, leading to a carbon distribution that is Rayleigh-Taylor unstable in the fluid surrounding the solid core. According to the estimates of Mochkovitch (1983; see also Isern et al. 1997), this unstable fluid mixes and homogenizes over short timescales compared to the cooling times. The net result is a partial separation between C and O after crystallization has occurred as compared to the initial distribution of these elements in the fluid phase, with the O/C ratio increasing with increasing depth. Given the large gravitational field operating in a white dwarf, the potential energy liberated owing to the partial sedimentation of the heavier element upon crystallization may significantly delay the cooling of the star. It should be understood here that the total amount of energy, ΔE , thus released remains quite small compared to the binding energy of the star, but the delay in cooling, Δt , can still be important because sedimentation occurs at low luminosities and $\Delta t \propto \Delta E/L$ (cf. Chabrier 1998). Even taking into account the effects of pre-white dwarf evolution which produce newborn white dwarfs with cores that are already O-enriched, Salaris et al. (1997) have found that

the subsequent separation leads to delays in the cooling times that are comparable in magnitude to the effects of the release of latent heat, although generally smaller.

The question of the exact relative distribution of C and O in the cores of white dwarfs at birth is of central importance in the description of the sedimentation process and, more generally, in the practical application of white dwarf cosmochronology. This problem was first investigated by Mazzitelli & D'Antona (1986a, 1986b, 1987), who studied the evolution of models with $M = 1, 3,$ and $5 M_{\odot}$ all the way from the main sequence to the white dwarf stage. More recently, in a very significant publication, Salaris et al. (1997) have reexamined this question of pre-white dwarf evolution with the help of more detailed and sophisticated calculations aimed at providing the initial chemical profiles in the cores of white dwarfs having main sequence progenitors in the mass range $1\text{--}7 M_{\odot}$. The chemical profiles obtained by Salaris et al. (1997) provide the best starting conditions currently available for the further evolution of C/O core white dwarfs. Unfortunately, because of existing uncertainties in the rates of He thermonuclear burning, there is no unique initial chemical profile for a white dwarf of a given mass; indeed, Salaris et al. (1997) have considered two extreme possibilities, one corresponding to a “high” rate for the $C^{12}(\alpha, \gamma)O^{16}$ reaction, and the other corresponding to a “low” rate. This gives rise to important differences; for example, their central value of the oxygen mass fraction in a newborn white dwarf with a total mass of $0.6 M_{\odot}$ is $X_O = 0.74$ for the high rate and $X_O = 0.57$ for the low rate. This uncertainty in the proportions and distributions of C and O in the cores of white dwarfs at birth constitutes currently one of the major limitations of the whole approach of white dwarf cosmochronology.

It should be pointed out that the white dwarf cooling calculations in the series of papers initiated by Garcia-Berro et al. (1988) suffer from some limitations of their own. In particular, they are all based on a method which compares the binding energies of *static* models which are assumed perfectly isothermal. Thus the benefits of computing full evolutionary models are forfeited in this approach, and the approximations that were used to go from equation (1) to equation (2) above are built-in. Furthermore, these structures are only C/O *core* models with no outer He or H/He envelopes, and it is necessary to use $L\text{--}T_c$ relations provided by independent model calculations (see eq. [2]). This approach necessarily introduces some inconsistencies in the calculations: those are (1) the chemical composition of the core of the models used to derive the $L\text{--}T_c$ relation differs from the *variable* core composition of the assumed isothermal structure that undergoes phase separation, (2) the relevant constitutive physics—namely, the equation of state of the fully ionized fluid/solid core—is generally different in the two sets of models, and (3) the core of a white dwarf is, of course, never strictly isothermal. The full series of papers based on the binding energy approach, and culminating with Salaris et al. (1997), uses the $L\text{--}T_c$ relation obtained from a

single evolutionary sequence computed by Wood & Winget (1989) for a $0.6 M_{\odot}$ star with an uniformly mixed C/O core ($X_C = X_O = 0.5$) and a helium outer layer containing 10^{-4} of the total mass of the star. Since the Wood & Winget (1989) sequence predates the era of the OPAL radiative opacities, this $L\text{--}T_c$ relation must be considered outdated. Furthermore, it applies only to non-DA stars, and not to DA objects which constitute the bulk of the white dwarf population. The effects of chemical layering on the luminosity–core temperature relation have been best described in Tassoul, Fontaine, & Winget (1990), and it is clear that there are very important differences between DA models with “thick” hydrogen layers and non-DA models, especially at low luminosities. Of greater concern still, is the use of $L\text{--}T_c$ relations for masses other than $0.6 M_{\odot}$ which have been simply *scaled* on the original Wood & Winget (1989) relation according to the value of the mass relative to $0.6 M_{\odot}$. We must point out that $L\text{--}T_c$ relations for white dwarfs do *not* scale well on the mass, as was already quite apparent in Fontaine & Van Horn (1976), for example. This is particularly true in the interesting regime where convective coupling enters into the picture and modifies considerably the slope of the $L\text{--}T_c$ relation as discussed below. Since convective coupling sets in at different luminosities for different masses and since it plays a major role in the evolution, the simple scaling strategy advocated in the series of papers initiated by Garcia-Berro et al. (1988) misses an effect that is of key importance in the calculation of the cooling time and in the evaluation of the white dwarf luminosity function. A major improvement on this front has been the work of Chabrier et al. (2000), who computed state-of-the-art $L\text{--}T_c$ relations for *several* different masses and folded them into cooling calculations. Within the inherent limitations of the binding energy method as described above, these latter calculations are arguably the most accurate cooling computations currently available.

Another significant theoretical development is due to Hansen (1999), who emphasized the importance of using detailed model atmospheres as surface boundary conditions in cooling calculations for old white dwarfs. This is in contrast to the standard use of gray atmospheres in all previous calculations carried out until then. As discussed initially by Fontaine et al. (1974) in a slightly different context, the most important consequence of such a detailed description of the atmosphere on the cooling problem is its effects on the location of the base of the convection zone in the deeper envelope. Indeed, it is well known in model atmosphere theory that, when it exists, the convection zone in a nongray atmosphere is shifted upward as compared to its location in the corresponding gray atmosphere. This results from the feedback effect of convection on the structure of the detailed atmosphere (see, e.g., Böhm et al. 1977 for a discussion of this phenomenon in a white dwarf context). The upward shift of the superficial convection zone in more detailed models—and indeed, the full atmospheric structure—has no consequence whatsoever on the cooling process, until the base of the superficial convection zone in an

evolving white dwarf reaches into the degenerate core, thus coupling, for the first time, the atmospheric layers with the thermal reservoir. Since, by then, the stratification of the envelope is fully convective and highly adiabatic, changes in the atmosphere produce corresponding changes at the base of the convection zone. The upward global shift of the convection zone in cooling models incorporating detailed atmospheric structures, and, in particular, the upward shift of the location of its base delays the onset of convective coupling. This, in turn, retards the release of excess energy that becomes available when the full envelope surrounding the thermal reservoir becomes as transparent as it can get (through an adiabatic convective stratification). Interestingly, this offset of convective coupling toward lower luminosities increases the cooling time by amounts that are comparable to those produced by C/O sedimentation in the core.

The approach to white dwarf cosmochronology advocated by Hansen (1999) is impressive in that he chose to develop a full evolutionary code that incorporates detailed model atmospheres and atmospheric opacities of his own, thus ensuring the internal consistency that is lacking in the binding energy method used by others. Hansen (1999) also included the effects of residual thermonuclear burning to set the mass-dependent maximum fractional mass of the outer hydrogen layer in his DA models. He was also able to push his calculations into the interesting regime of very low effective temperatures ($T_{\text{eff}} \lesssim 4000$ K) without, apparently, resorting to the extrapolation trick used by Wood (1990, 1992, 1995), for example. Despite these achievements, his work has been criticized by Isern et al. (2000), who drew attention to the facts that Hansen's treatment of the thermodynamics of the dense Coulomb plasma of the core is only rough at best and that his description of the effects of C/O sedimentation upon crystallization underestimates seriously the magnitude of the associated time delay. Thus, even though Hansen (1999) has developed, at least in principle, the best approach so far to the problem of cooling white dwarfs, it appears that substantial improvements at the level of the microphysics are required in his calculations.

The computations of more realistic and sophisticated model atmospheres for cool white dwarfs constitute also an essential development on the road to white dwarf cosmochronology. Not only are these models needed for providing more realistic surface boundary conditions for cooling calculations as discussed just above, they are also obviously necessary for computing emergent fluxes with which to interpret the observed spectra and colors. The current standards for model atmospheres and photometric colors of cool white dwarfs of both the DA and non-DA types have been provided in the series of papers by Bergeron, Wesemael, & Fontaine (1991), Bergeron, Saumon, & Wesemael (1995a), and Bergeron, Wesemael, & Beauchamp (1995b). While these models are sufficient for analyzing disk white dwarfs, they do not extend to effective temperatures lower than $T_{\text{eff}} = 4000$ K. In the light of the exciting suggestion of Chabrier, Segretain, & Méra (1996; see also Hansen 1998)

for the existence of an ancient population of white dwarfs in the Galactic halo (the DA objects being still visible in the Hubble Deep Field), the need for even cooler models became evident. In this context, Hansen (1998, 1999) computed his own set of model atmospheres for both DA and non-DA stars extending to effective temperatures lower than 4000 K, into the regime of interest for halo and Galactic cluster white dwarfs. More detailed model atmospheres for DA white dwarfs were also presented by Saumon & Jacobson (1999) in the range $4000 \text{ K} \geq T_{\text{eff}} \geq 1500 \text{ K}$.

In concluding this subsection, we note that a comparison of the available estimates of cooling timescales obtained by various groups (including other recent efforts based on full evolutionary codes such as those of Benvenuto & Althaus 1999; Montgomery et al. 1999; and Salaris et al. 2000) shows a spread of values that is, at the very least, somewhat uncomfortable. At first sight, this casts a shadow on our ability to use white dwarf cosmochronology as a quantitative science. However, much of the spread is likely due to a number of different approximations in the model-building phase and of different choices of model parameters and generations of input microphysics between the various groups. Thus, we feel that there are no "fundamental" limitations intrinsic to the cooling models and that there is every reason to be optimistic about the ultimate usefulness of white dwarf cosmochronology. Indeed, building on the strengths of the milestone papers we briefly described here, and trying to avoid their limitations, we point out that there is still plenty of room for improvements that should allow researchers, ultimately, to obtain very accurate cooling times. In this spirit, we, along with other groups, have embarked on the computations of such improved cooling models. In the present paper, we use some of our own initial results to describe representative behaviors of cooling white dwarfs.

3.2. Results from Recent Calculations

We have developed a completely new evolutionary code based on very efficient finite-element techniques. While the details of that code will be described elsewhere (P. Brassard & G. Fontaine 2001, in preparation), a few remarks about it are worthy of interest. The code has been especially designed to handle in a robust and accurate way (1) the crystallization process (i.e., the moving boundary of the crystallization front, the release of latent heat, and the redistribution of elements between the liquid/solid phases), (2) diffusion of the various atomic species, (3) convective mixing, and (4) nuclear processes (i.e., residual thermonuclear burning and neutrino emission mechanisms). A key feature of our code is that the *full* structure of a model, from the center to the top of the atmosphere (typically located at $\tau_R = 10^{-8}$), is included in the evolutionary calculations. This is of importance for an accurate description of convective coupling (see below) and, of course, is essential for following the advancing crystallization front in both the C/O core *and* the H/He envelope. Such an approach

is also required for including residual gravitational contraction of the envelope, a phenomenon that has some importance in the very low luminosity phases of the evolution of white dwarfs. It must also be used in the context of the spectral evolution of white dwarfs and, in particular, for following the time history of the composition transition zones that separate the various chemical layers in a typical, nonhomogeneous, stratified white dwarf. To complement this detailed approach to the evolution of white dwarfs, we have also computed new improved model atmospheres that now extend down to $T_{\text{eff}} = 1500$ K. Complete new grids were computed using the input physics described in Bergeron et al. (1995a) and incorporating the improvements discussed in Bergeron, Ruiz, & Leggett (1997) and in Bergeron, Leggett, & Ruiz (2001). These latest models provide a homogeneous set of photometric colors covering the full range of effective temperatures of interest, including the regime of very low luminosity white dwarfs. We also use the structures of these detailed model atmospheres as an optional choice for the surface boundary conditions of our evolutionary models. The other option is the use of standard gray atmospheres, as has been used in *all* evolutionary calculations carried out so far, with the exception of those of Hansen (1999), of Salaris et al. (2000), and, in the particular case of He-core, low-mass white dwarfs, of Aparicio & Fontaine (1999).

The constitutive physics currently included in our evolutionary code consists of four large tables of thermodynamic data, one for each species of interest (H, He, C, and O). Each equation-of-state table is made of three parts corresponding to different regions of the ρ - T plane. For the first region, of primary relevance in the atmosphere and in the upper envelope of the hotter models, the equation of state is obtained by solving the appropriate network of Saha equations which include a small correction term for the Coulomb interaction. The second part is the region of partial ionization and partial degeneracy that covers approximately the envelope. For the H and He species, we use the Saumon, Chabrier, & Van Horn (1995) data. For the C species, we use an improved unpublished version of the equation of state of Fontaine et al. (1977). The O equation of state is cruder and is given by the solution of the Saha equations with a Coulomb term and a pressure ionization term from Eggleton, Faulkner, & Flannery (1973). In the last region, corresponding to the completely ionized interior, we use the detailed thermodynamic data of Lamb (1974) with some improvements of our own in the electronic terms. The code of Lamb (1974) provides a complete description of the liquid and solid phases, including the calculation of the latent heat upon crystallization. For the radiative opacities, we use the OPAL 1995 data from Iglesias & Rogers (1996) for pure substances. At low temperatures, where the OPAL data are not available, we use our own Rosseland opacities for pure H and pure He that we computed from our model atmosphere codes. These calculations take into account detailed absorption processes, including the H quasi-molecular opacity of Allard et al. (1994)

and a number of collision-induced absorption processes as described in Bergeron et al. (1995a; see also Bergeron et al. 1997, 2001). The conductive opacities combine the low-density data of Hubbard & Lampe (1969) with the high-density results of Itoh et al. (1983, 1984; Itoh, Hatashi, & Kohyama 1993; Itoh & Kohyama 1993), the latter covering both the liquid and solid phases. Data are available on option both for pure substances (the usual choice) and for mixtures containing small traces of heavy elements. The phase diagram that we currently use for the process of C/O sedimentation upon crystallization is that of Segretain & Chabrier (1993). The diffusion coefficients are those of Paquette et al. (1986). The thermonuclear reaction rates for hydrogen residual burning are taken from Fowler, Caughlan, & Zimmerman (1975). The neutrino emissivities are taken from Itoh et al. (1996). Finally, we have a number of options to treat convection within the general framework of the mixing-length theory. Note, however, that the usual uncertainties associated with that approach are of no consequence on the calculation of the cooling time of a white dwarf because, by the time convective coupling sets in, the stratification in the superficial convection zone has become entirely adiabatic (see, e.g., Tassoul et al. 1990 for a more detailed discussion of this).

We have recently completed the computations of a first family of evolutionary models designed to serve as reference structures and templates. In particular, in order to study the various effects of the inclusion of more sophisticated descriptions, we considered basic structures comparable to those of Wood (1995), since the latter have remained the most accessible standards in the field. Thus, we computed standard “thick-envelope” DA stellar models with a He mantle containing 10^{-2} of the total mass of the star, and an outermost H layer containing 10^{-4} of the total mass of the star. The core of these models consists of pure C. The metal content is zero ($Z = 0$) throughout the star. As in Wood (1995), we assumed gray atmospheres as surface boundary conditions, and we assumed diffusive equilibrium in the H/He and He/C transitions zones (and, thus, diffusion was turned off). Furthermore, the layers of H and He are sufficiently thick that no convective mixing can occur in these models. No residual thermonuclear burning has been included in order to keep the same value— 10^{-4} —of the fractional mass of the outer H layer in all models. In contrast, neutrino cooling has been included, but this affects only the evolution in the high-luminosity phases only, as is well known. The choice of a pure composition in the core precludes, of course, sedimentation of species during the crystallization process. Finally, 23 different masses have been considered, in the range 0.2 – $1.3 M_{\odot}$ and in steps of $0.05 M_{\odot}$ in order to provide sufficient resolution in the calculation of the theoretical luminosity function. On purpose here, this mass range exceeds the range (~ 0.45 to $\sim 1.1 M_{\odot}$) in which *real* C/O core white dwarfs are expected to be found. For low masses, white dwarfs with He cores are expected to be found, while for $M \gtrsim 1.1 M_{\odot}$, white dwarf stars should have O/Ne cores (Garcia-Berro, Isern, & Hernanz 1997).

It should be clear that the models belonging to this first family are not the most realistic and most sophisticated that we can calculate. The latter are being currently computed and will become available in the near future, we hope. Nevertheless, our template models are perfectly suitable for the illustrative applications of white dwarf cosmochronology that we consider below in this paper. We warn the reader, however, that the ages of the various white dwarf populations that we derive here are not our “definitive” answers or “best-guessed” values. In this context, it is appropriate to point out that the choice of a pure C core composition is not totally arbitrary. Indeed, even in the presence of the retarding effect of element sedimentation in a more realistic C/O core undergoing crystallization, the cooling time remains smaller than that of a pure C core object, all other things being the same. This implies that, within the limitations imposed by our choice of parameters in the computations of our reference models, the derived ages obtained here are *upper limits*.

A first insight into the physics of cooling white dwarfs is obtained by studying the evolution of the structure of a representative model in a phase diagram. We provide an example in Figure 1 which illustrates how the ρ - T structure relation of a typical $0.6 M_{\odot}$ DA model changes with cooling, from an initial effective temperature of 35,000 K to a final value of 2000 K. Here, the logarithmic scales emphasize the atmosphere/envelope regions which are quite opaque, but also quite thin. The vertical dashed curves define the locations of the H/He and He/C transitions zones; even though the C core covers only a small portion of each curve at the right end, it nevertheless contains 99% of the total mass of the star. We have indicated the position of the degeneracy boundary in each model, defined here as the location where the value of the usual electron degeneracy parameter, η (ηkT is the chemical potential of the free electrons), equals 0. This is given by the small filled circle along each curve; to the right of that position, the value of η is positive and keeps increasing with increasing depth. Likewise, the larger open circle along each curve defines the position in the star where Γ , the usual Coulomb coupling parameter (the ratio of the typical Coulomb potential energy of an ion to its average kinetic energy kT), is equal to 1. This loosely defines the transition between the gaseous and liquid states in the white dwarf. It can be easily seen that, as the direct result of cooling, both the degeneracy boundary and the gas/fluid boundary are pushed up into the star, to the point where, in the coolest models, conductive transport and fluid physics become relevant to the description of the atmospheric layers. This shows, at least in part, why the computations of realistic model atmospheres for cool white dwarfs are not trivial. We also point out that, even for the hottest model considered here ($T_{\text{eff}} = 35,000$ K), the full C core is in the liquid state, meaning that treating its thermodynamics in terms of a perfect gas (as done within the framework of the Mestel theory, for example) is a poor approximation. Of course, the ions become more strongly correlated with cooling and, by the time Γ reaches a value of ~ 180 (a value derived from detailed Monte Carlo simulations),

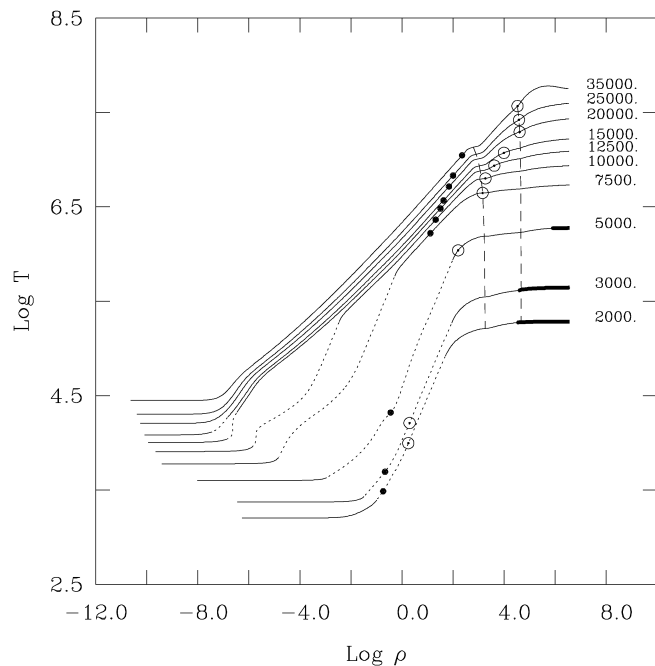


FIG. 1.—Evolving structure of a representative model of a DA white dwarf in a phase diagram. This model has a mass of $0.6 M_{\odot}$ and belongs to our family of 23 reference models. Each curve corresponds to the density-temperature distribution from the surface (defined here by the location of optical depth $\tau_r = 10^{-8}$) to the center of the model at an effective temperature given by the number alongside. The solid, dotted, and thick solid (for the three cooler epochs) portions of each curve indicate the radiative-conductive, convective, and crystallized regions. The top of the convection zone is always located in the photospheric layers. Electrons become degenerate to the right of the small filled circle on each curve. Likewise, the bigger open circle on each curve indicates the location to the right of which the ions become strongly correlated (fluid phase). The dashed curves define the composition transition zones, H/He at lower densities, and He/C at higher densities.

crystallization sets in. The thick solid portions of the curves corresponding to the three coolest models illustrated here show indeed how a crystalline nucleus grows from the center outward. At the end of the sequence, when the white dwarf has reached an effective temperature of 2000 K, more than 99% of the mass of the star has solidified.

There are at least three modes of energy transport that are relevant to evolving white dwarfs. Conduction is the dominant mode in the degenerate core, which, as we have seen, grows with cooling. This leads to a flattening of the temperature distribution in the deep interior, but Figure 1 clearly shows that a white dwarf interior is never strictly isothermal. A detailed description of conductive opacities in both the liquid and solid phases is thus an essential ingredient for an accurate description of cooling white dwarfs. Radiation dominates in the nondegenerate envelope of hot stars. In fact, at high enough effective temperatures, the outer layers are fully ionized and radiative and possess the same character as the so-called radiative-zero solutions of Schwarzschild (1958). This means that the evo-

lution is completely insensitive to the details of the outermost layers, including, in particular, the atmosphere (assumed gray or otherwise). However, as discussed at length in Tassoul et al. (1990), a precise knowledge of the radiative opacity is still needed in the deeper envelope, where radiation and conduction have comparable efficiencies. With further cooling, the element in the superficial layers (H in the present example) recombines, which increases considerably its radiative opacity. The temperature gradient in the surface layers must then also increase, and, in response, the gas/fluid matter becomes ultimately unstable against bulk convective motions. Thus, a superficial convection zone develops, mapping the region of partial ionization of H in our example. This is shown in Figure 1 by the dotted curve segments in models with T_{eff} equal to 15,000 K and lower. From that point on, atmospheric convection leaves its signature on the emergent flux and is therefore an essential ingredient for interpreting observed spectra and photometric colors. However, it is only when the base of the superficial convection zone reaches into the reservoir of thermal energy—and this corresponds roughly to the boundary of the degenerate core—that, for the first time, the surface becomes directly coupled to that reservoir. When that happens, i.e., when the envelope is fully convective from the photosphere down to the upper boundary of the thermal reservoir, the subsequent evolution becomes sensitive to the details of the atmospheric layers. This is because the convective stratification has become essentially adiabatic. Convective coupling has thus occurred in models cooler than $T_{\text{eff}} = 7500$ K in Figure 1. Note that a precise knowledge of the *radiative* opacity is still very much needed in these cooler models in order to determine the exact locations of the top and base of the convection zone.

Another instructive view of the properties of cooling white dwarfs is provided by Figure 2, which illustrates the evolutionary tracks of five of our template models (differing only by their mass) in the Hertzsprung-Russell (HR) diagram, as well as representative isochrones (*thick solid curves*). Because of the peculiar mass-radius relation characterizing degenerate stars as alluded to above, the more massive white dwarfs are also those that are the smaller, and this is clearly shown by the evolutionary tracks. It is also obvious that these paths nearly follow curves of constant radii (straight lines with a slope of -4 in this log-log version of the HR diagram). This is particularly true for the more massive, collapsed objects and also at low luminosities where residual gravitational contraction has practically ceased. We have indicated, along each track, 3 important epochs in the cooling history of a white dwarf. First, the open circles at high luminosities (two of which are off-scale and, therefore, not shown) loosely define the transition between the neutrino cooling phase at higher luminosities and the thermal cooling phase at lower luminosities. The circles correspond to the epoch when the neutrino luminosity, previously dominant, becomes equal to the photon luminosity. In the early, short-lived phase of evolution following immediately the planetary nebula phase, white dwarf interiors are still hot

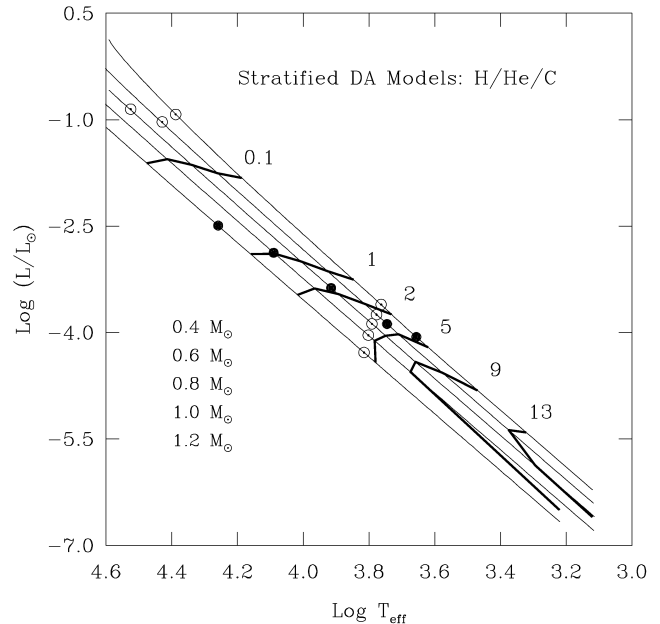


FIG. 2.—Evolutionary tracks (*solid curves*) of five ($M = 0.4, 0.6, 0.8, 1.0,$ and $1.2 M_{\odot}$, from top to bottom) of our reference models of DA white dwarfs in the Hertzsprung-Russell diagram. The thick solid curves are isochrones. The number next to each isochrone gives the cooling time in units of Gyr. The small filled circles indicate the onset of crystallization at the center of each evolving model. The larger open circles at high luminosities indicate the transition between the neutrino cooling phase (which dominates at higher luminosities) and the thermal cooling phase (which becomes relevant at lower luminosities). The other set of open circles at lower luminosities indicates the onset of convective coupling between the surface and the thermal core.

enough that neutrinos can be formed in great quantities there through a number of processes involving the electroweak interaction. The vast majority of the neutrinos escape directly from the central regions where they are created to the outer space, thus contributing to an important stellar energy sink. For instance, neutrino luminosities may become 2 orders of magnitude larger than photon luminosities in these objects. The evolution of a very hot, young white dwarf is thus dominated by neutrino cooling. Neutrino processes largely specify the cooling timescale of a very hot white dwarf and lead as well to a temperature reversal in the stellar core. Such a reversal is still visible in the hotter model shown in Figure 1, for example. By the time a $\sim 0.6 M_{\odot}$ white dwarf has cooled down to $T_{\text{eff}} \sim 25,000$ K, however, the star has lost its memory of the neutrino cooling phase and enters the thermal cooling phase proper. Its subsequent evolution and structure depend exclusively on the properties of its degenerate electrons and thermal ions.

The second set of open circles attached to the evolutionary tracks at much lower luminosities indicate the onset of convective coupling, i.e., the epoch when the base of the superficial H convection zone in these models first reaches the upper boundary of the degenerate core ($\eta = 0$). From that point on, as explained above, convection affects directly the rate of cool-

ing of a model since it transports energy through the outermost insulating layers more efficiently than would be possible through radiative-conductive transfer alone. The third epoch of interest is the onset of crystallization at the center of each evolving model; this is indicated by the small filled circles on the tracks. We note that because of their larger masses *and* smaller radii, more massive white dwarfs have larger internal densities (for comparable temperatures) and, therefore, develop a crystallized core earlier, at higher luminosities or, equivalently, higher effective temperatures. Figure 2 also shows that more massive models undergo a relatively rapid and final phase of cooling toward the black dwarf state at the cool end of the sequence. This produces the dramatic bending of the late isochrones in the figure. This is due to the fact that more massive stars also reach earlier the state where the specific heat in the solid regime plunges to very small values, a phenomenon well understood within the framework of the simple Debye theory of solids in quantum statistical mechanics. In effect, matter under these conditions has lost much of its ability to store thermal energy, the energy reservoir of a white dwarf has become nearly empty, and the star must then disappear from sight in a relatively rapid phase often referred to as “Debye cooling.” Crystallization and subsequent Debye cooling are responsible for the “accelerated” evolution of the more massive models at low luminosities. In contrast, at much higher luminosities, before crystallization has set in, but after neutrino cooling has subsided, Figure 2 illustrates a more “normal” behavior: A more massive white dwarf takes longer to cool to a given effective temperature (say) than a less massive object. This is simply because the more massive star has a larger energy reservoir, with more C ions with energy kT . Overall, the isochrones shown in Figure 2 clearly demonstrate that the cooling time of a white dwarf is a strong function of both its luminosity (effective temperature) and its mass.

It should be realized that, despite the generalized use of the term “Debye cooling,” the actual thermodynamic description employed in modelling white dwarf interiors is much more sophisticated than the simple Debye approach (see, e.g., Lamb 1974 or Chabrier 1993). In this context, Figure 3 illustrates the behavior of the specific heat (per gram) at the center of the five evolving models described in the previous HR diagram. Each curve shows the central value of the specific heat for a given model of fixed total mass as a function of the central temperature; hence, evolution proceeds from right to left along a specific curve. Note that the central density of each evolving model does not practically change during the evolution. The small filled circle on a given curve indicates the location of the phase transition from the liquid to the solid state. A discontinuity in C_{ve} , particularly pronounced in the more massive model, is associated with this (first-order) phase transition. For comparison, the dotted curve gives the behavior of the central specific heat for a simple model of a $1.2 M_{\odot}$ solid star constituted of pure ionized (metallic) carbon with the ion lattice treated as a Debye solid and the electrons treated as a perfect

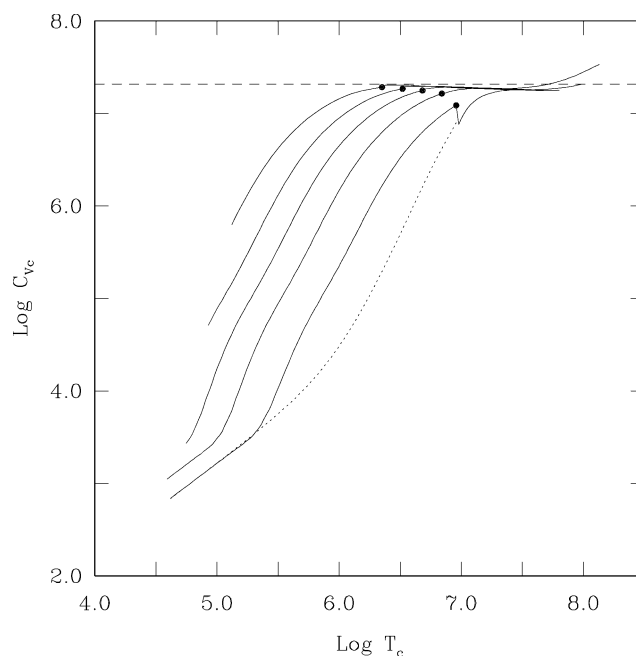


FIG. 3.—Evolutionary tracks (*solid curves*) of five ($M = 0.4, 0.6, 0.8, 1.0,$ and $1.2 M_{\odot}$, from top to bottom) of our reference models of DA white dwarfs in the central specific heat–central temperature diagram. The evolution proceeds from hot to cold along each track. The small filled circle on a track indicates the onset of crystallization. The dotted curve illustrates the behavior of a $1.2 M_{\odot}$ model treated within the framework of the simple Debye theory of solids. The horizontal dashed curve gives the value of the specific heat (per gram) for a pure C solid in the classical regime.

degenerate Fermi-Dirac gas. At sufficiently high temperatures for the classical description to be appropriate, the specific heat of such a simple system is given by the Dulong-Petit law, i.e., the *constant* value shown by the horizontal dashed curve in the figure. However, as is well known, quantum effects become of importance at low temperatures, and, in particular, when the temperature of the solid becomes much smaller than the so-called Debye temperature (a characteristic value that actually measures the density of the ions), the thermal motions of the ions contribute a term to the specific heat that is now proportional to T^3 . This term dominates until the temperature drops to such low values that the sole remaining capacity for the star to store thermal energy is through the weak contribution of degenerate relativistic electrons ($C_v \propto T$). The dotted curve in Figure 3 illustrates perfectly the transition from the regime where the slope is equal to 3 at intermediate temperatures to the regime where the slope is equal to 1 at very low temperatures. We note that there are very large quantitative differences between the specific heat of the actual $1.2 M_{\odot}$ model and that predicted through the Debye model, implying that a detailed treatment of the thermodynamics of the solid (and of the liquid, of course) is absolutely required, as was realized initially by Lamb (1974). Nevertheless, all the models shown here exhibit a Debye-like behavior in their specific heat. Ultimately, this

plunge of the specific heat precipitates them to the black dwarf state.

More can be learned about the characteristics of evolving white dwarfs by examining the so-called cooling curve of a model, that is, a plot of the cooling time, t_{cool} , as a function of the luminosity, L . An example is provided by the solid curve in Figure 4, which refers to the most massive star ($1.3 M_{\odot}$) in our family of template models. The curve shows clearly that there are two distinct epochs when delays in the cooling time are produced. These delays are associated with the two major events alluded to above, namely, the onset of crystallization and the onset of convective coupling. These phenomena occur in all of our models, but we chose here an atypical mass of $1.3 M_{\odot}$ in our illustration because crystallization and convective coupling set in at quite different times in this particular model and, therefore, are well separated, do not overlap, and can be easily distinguished in the cooling curve. As will be seen below, this is not the case for a model with a more typical mass of $\sim 0.6 M_{\odot}$. The first delay in the cooling curve is correlated with the onset of crystallization, as can be easily seen by examining the dashed curve in the figure. The latter shows the position of the upper boundary of the growing solidified portion of the star. The delay in cooling time is produced by the release of latent heat upon crystallization in a first-order liquid-to-solid phase transition. Of course, this release of energy is gradual; it begins immediately after crystallization sets in at the center of the star and continues to be of importance until most of the mass of the model has solidified. Figure 4 shows that the net effect on the cooling curve is quite significant. Indeed, the slowdown in the cooling process clearly manifests itself through the obvious change of slope in the cooling curve near $L/L_{\odot} \approx 10^{-1.9}$. We note, parenthetically, that our code allows us to follow realistically the progress of the crystallization front not only in the C core but also all the way into the He/H envelope. The plateau portions of the dashed curve correspond to retardations of the progression of the front across a composition transition zone since the reduced Coulomb coupling produced by the decreased charge of the lighter element above the transition zone must be compensated by a lower temperature. At the end of the sequence, in our coolest model, some of the hydrogen is already in the solid metallic form, and more than 99.99% of the mass of the star has crystallized.

The second delay in the cooling process, of higher magnitude than the first one and associated with the change of slope in the cooling curve near $L/L_{\odot} \approx 10^{-4.5}$, is due to the onset of convective coupling. Indeed, the bump structure in the cooling curve is tightly correlated with an important change of slope in the dotted curve in Figure 4. The latter curve shows how the central temperature of the model is related to the luminosity (the L - T_c relation mentioned above). The change of slope occurs precisely when the envelope becomes fully convective, i.e., when convection first breaks into the thermal reservoir. There is a change of slope because convection flattens the temperature

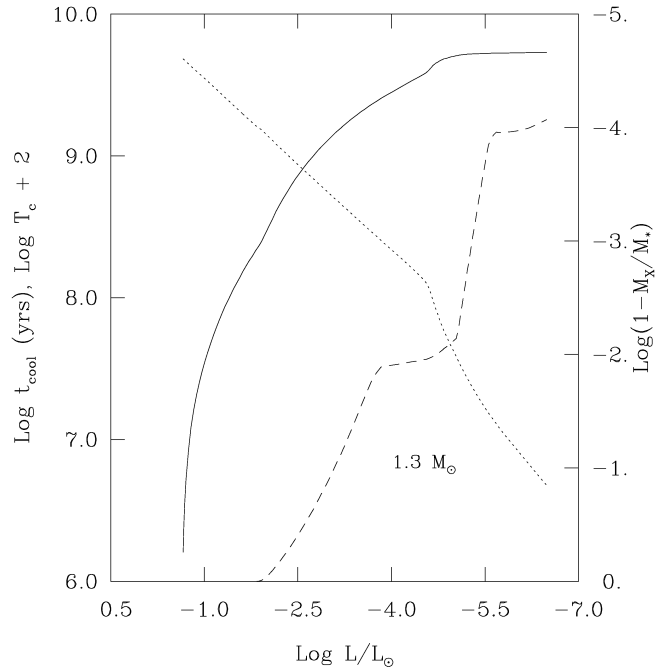


FIG. 4.—The solid line shows the cooling curve ($\log t_{\text{cool}}$ vs. $\log L/L_{\odot}$) of a $1.3 M_{\odot}$ model. The dashed curve shows the progression of the advancing crystallization front from the center to the base of the H outer layer. The position of that front is expressed in terms of fractional mass depth as read on the right-hand-side scale. The plateau sections of the curve correspond to the composition transition zones; the C/He zone located near $\log(1 - M_x/M_*) \approx -2.0$, and the He/H zone located higher in the star, near $\log(1 - M_x/M_*) \approx -4.0$. The dotted curve illustrates the L - T_c relation of the model.

gradient as compared to purely radiative models. Until that moment in time, the thermal reservoir remains relatively well insulated by at least that part of the nondegenerate envelope that is still radiative and opaque, but, when convection finally breaks completely through that barrier, the full envelope becomes significantly more transparent and there is, initially, an excess of thermal energy that the star must get rid of. This release of excess energy slows the cooling process down for a while and produces a delay, a bump in the cooling curve. It should be understood, however, that once the excess of energy is liberated, convection has just the opposite effect, i.e., it *speeds up* the cooling process with respect to models that would have purely radiative envelopes because the thermal reservoir is now less well insulated than before. In this context, the dotted curve in Figure 4 illustrates remarkably well the very important cooling effect of adiabatic convection on the central temperature *once convective coupling has been achieved*. Models in forced radiative equilibrium would predict significantly higher values of T_c in low-luminosity stars, values that would fall on an extension of the high-luminosity segment of the L - T_c relation that forms a line with an almost constant slope in the figure.

It is instructive to examine again, but from a slightly different and complementary point of view, this question of delays in

the cooling time and to consider as well the dependence on the mass of the star. This time, we show, in Figure 5, not the cooling curve itself, but its derivative, which is a more sensible way to illustrate the effects of crystallization and convective coupling on the cooling time. Actually, we plotted the derivative of t_{cool} with respect to the bolometric magnitude, M_{bol} , as a function of the luminosity. To within a constant, this is, of course, equivalent to the derivative of the cooling curve. Our choice is motivated by the fact that the derivative $dt_{\text{cool}}/dM_{\text{bol}}$ is used directly in the calculation of the theoretical luminosity function (see eq. [4] below). We note that this quantity is the inverse of the cooling rate. The curves in Figure 5 illustrate the behavior of this quantity for 12 of our template models spanning the full range of mass considered in our calculations, from $0.2 M_{\odot}$ (at the top) to $1.3 M_{\odot}$ (at the bottom) in steps of $0.1 M_{\odot}$. Only the $0.2 M_{\odot}$ curve has the correct ordinate; the others have been shifted arbitrarily downward by 0.4 dex for each increment of $0.1 M_{\odot}$ in mass in order to facilitate the visualization process. Along each curve, cooling proceeds from left to right, and the general behavior with decreasing luminosity is an initial increase of $dt_{\text{cool}}/dM_{\text{bol}}$, culminating at a maximum associated with a delay process (when the cooling rate is at its minimal value), and followed by a decrease due to Debye cooling. In this latter phase, and for the more massive stars, the cooling rate can reach values as large as those obtained during the high-luminosity, short-lived neutrino cooling phase. The first open circle along an evolutionary track indicates the onset of crystallization at the center of the model. The delay in cooling due to the subsequent release of latent heat manifests itself in terms of an obvious structure in each curve. By the time 98% of the mass of the star has crystallized, an epoch indicated by the second open circle along a curve, most of the latent heat has been released. As already shown in Figure 2, we again observe here that crystallization occurs at higher luminosities for more massive stars. Moreover, we find that the process of latent heat release covers a wide range of luminosities over the mass spectrum considered in the present example. In contrast, the delay in cooling associated with convection breaking into the degenerate thermal reservoir arises at higher luminosities for the less massive stars and, in addition, occurs in a narrower range of luminosities. It also produces a structure in the $dt_{\text{cool}}/dM_{\text{bol}}$ versus L curve that is generally larger than that caused by latent heat release. The actual epoch of the onset of convective coupling is indicated on each curve by the small filled circle preceding immediately the structure associated with the release of excess thermal energy. As above, the symbol identifies the one model along a sequence for which the base of the superficial H convection zone first reaches the upper boundary of the degenerate core.

An unexpected result of our calculations is the realization that the release of excess thermal energy associated with convective coupling leaves a signature on the theoretical luminosity function (via its effects on $dt_{\text{cool}}/dM_{\text{bol}}$) that is actually *larger* than that caused by the release of latent heat upon crystallization. The

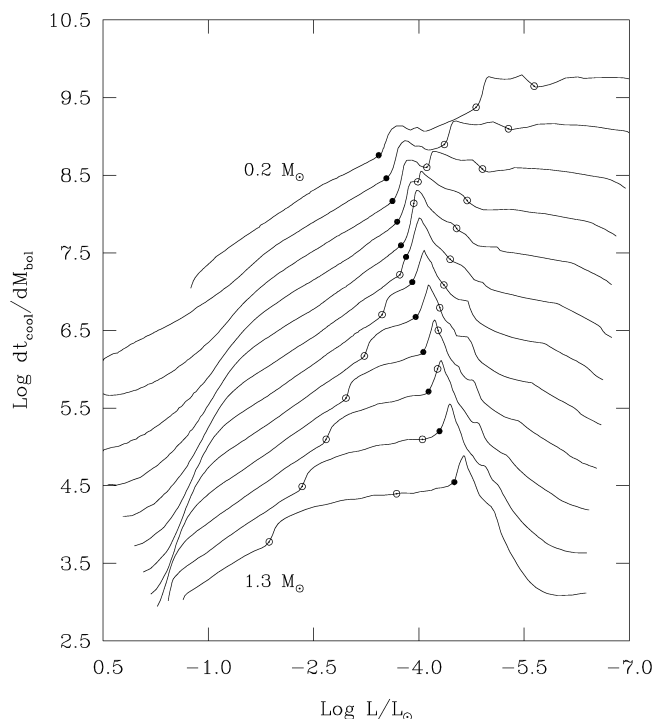


FIG. 5.—Evolutionary paths (solid curves) of 12 ($M = 0.2, 0.3, 0.4, 0.5, 0.6, 0.7, 0.8, 0.9, 1.0, 1.1, 1.2,$ and $1.3 M_{\odot}$, from top to bottom) of our template models in a diagram showing the derivative of the cooling curve (to within a constant) as a function of the luminosity. Only the $0.2 M_{\odot}$ curve is on the correct vertical scale; the other curves have been arbitrarily shifted downward for visualization purposes. The first open circle (at higher luminosity) on each curve corresponds to the onset of crystallization at the center of the evolving model, and the second one indicates the epoch when 98% of the mass of the star has solidified. For its part, the small filled circle indicates the onset of convective coupling.

surprise comes from the fact that this very important finding has been missed in *all* previous discussions of white dwarf cooling theory. There are, however, historical reasons to explain, at least in part, this state of affairs, and we now know that our result is the direct consequence of having been able to model properly the *evolving* envelope within our new evolutionary code, as opposed to the more standard use of *static* envelopes in the other codes that have been used to address the white dwarf cooling problem. In the original computations of Lamb & Van Horn (1975), both the effects of crystallization and convection happened accidentally to overlap in time, causing a single delay feature in the cooling curve of their $1 M_{\odot}$ pure C model. Although the overlap was recognized by the authors, they had no way to untangle the individual effects of each mechanism. Furthermore, because they used static envelopes, the magnitude of the effects due to convective coupling was underestimated in their calculations, and they concluded, actually correctly, that the release of latent heat was the dominant retarding effect in their calculations. Unfortunately, as if some cosmic conspiracy were at work, this accidental overlap translates to more realistic

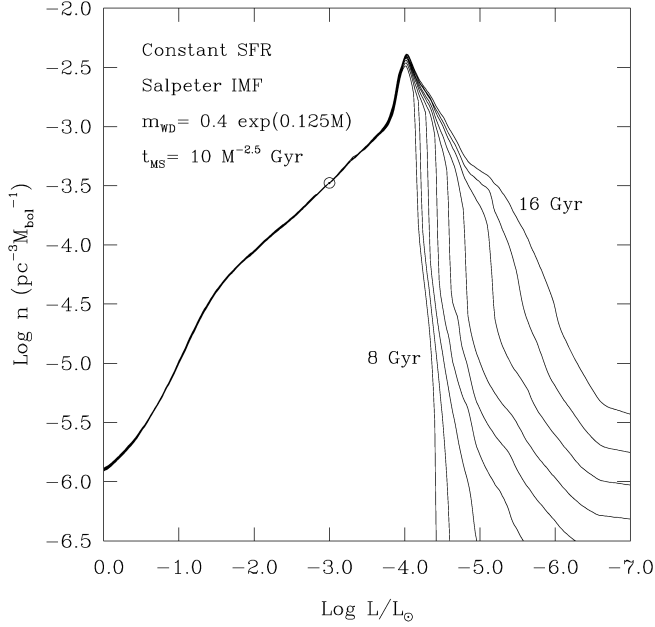


FIG. 6.—Examples of luminosity functions calculated for a model of the Galactic disk. The assumed age of the disk varies from 8 to 16 Gyr in steps of 1 Gyr. The curves are normalized at an arbitrary point indicated by the small open circle. The shape of the curves shows practically no dependence on the age on the ascending branch, but a very strong one at low luminosities.

chemically stratified models with representative masses around $\sim 0.6 M_{\odot}$, as is plainly evident in Figure 5 where the two “bumps” indeed overlap for models with intermediate values of the mass. Under these circumstances, it is easy to understand why previous investigators have interpreted the single delay feature seen in the cooling curve of a typical model in terms of a single cause (crystallization in the present case). When the standards of white dwarf cosmochronology were redefined by Wood (1990, 1992, 1995) in the early nineties, the importance of convective coupling was again underestimated because of his use of static envelopes, a computing strategy that is inherent to most evolutionary codes, including the Lamb (1974) code used by Wood. Thus, a bias against the effects of convection on the theoretical luminosity function was developed over the years, and several papers were published emphasizing uniquely the effects of crystallization. As we have seen here, only full evolutionary codes that include the complete structure, from the center to the upper atmosphere, are able to model properly time-dependent envelope effects and, in particular, the phenomenon of convective coupling which is of key importance for computing realistic luminosity functions. Interestingly and fittingly enough, the importance of convective coupling was foreseen by Tassoul et al. (1990), who also developed and used a code incorporating the evolution of the full model structure, including the envelope/atmosphere, but this was largely ignored.

It should be clear by now that one of the basic steps toward white dwarf cosmochronology is the evaluation of the theo-

retical luminosity function, to which we now turn. As is well known (see, e.g., Noh & Scalo 1990 for a particularly useful discussion of the question), the differential luminosity function of a white dwarf population in a stellar system of age t , i.e., the expected number of white dwarfs in the system with luminosity L , per unit bolometric magnitude, per cubic parsec is given by

$$n(L) = \int_{M_l}^{M_u} \frac{dt_{\text{cool}}}{dM_{\text{bol}}}(L, M[m_{\text{wd}}]) \times \psi[t - t_{\text{cool}}(L, M[m_{\text{wd}}]) - t_{\text{ms}}(M)] \times \phi(M)dM, \quad (4)$$

where the integration is carried out over the mass, M , of the white dwarf progenitor on the main sequence. The upper limit, M_u , is set by the statistics of neutron-star-forming main-sequence stars, currently $\sim 8 M_{\odot}$. The lower limit, M_l , is a function of the luminosity and is obtained by the condition

$$t_{\text{cool}}(L, M_l[m_{\text{wd}}]) + t_{\text{ms}}(M_l) = t, \quad (5)$$

where $t_{\text{cool}}(L, M[m_{\text{wd}}])$ is the cooling time to luminosity L of a white dwarf with a main-sequence progenitor of mass M , $t_{\text{ms}}(M)$ is the main sequence lifetime of that progenitor, and $M[m_{\text{wd}}]$ is the initial-to-final mass relation (IFR) tying a white dwarf of mass m_{wd} to its progenitor of mass M . Equality (5) reflects the fact that the oldest possible white dwarf at luminosity L has a *total* age equal to the age of the stellar system itself. Progenitors with masses less than M_l evolve so slowly on the main sequence that their white dwarf descendants have not yet had the time to cool to luminosity L in time t . In equation (4), $dt_{\text{cool}}/dM_{\text{bol}}$ is the inverse of the cooling rate as discussed above, ψ is the time-dependent stellar formation rate (SFR), and ϕ is the initial mass function (IMF). To illustrate some examples of actual computations of $n(L)$, we adopted from Wood (1990) analytic models for the various components entering equation (4). Thus, as appropriate for a discussion of the white dwarf population in the Galactic disk for example, we assumed a constant SFR, $\psi = \text{constant}$. Furthermore, we assumed a classic Salpeter IMF, $\phi = M^{-2.35}$, an IFR given by $m_{\text{wd}} = 0.4e^{0.125M}$, and a main-sequence lifetime law given by $t_{\text{ms}} = 10M^{-2.5}$ Gyr. In these expressions the masses M and m_{wd} are expressed in solar units. We also assumed that $M_u = 8 M_{\odot}$, implying, through the adopted IFR, that the maximum white dwarf mass in the disk is equal to $1.087 M_{\odot}$ (for single-star evolution). Finally, we used our full grid of 23 evolutionary sequences to generate the $dt_{\text{cool}}/dM_{\text{bol}}(L, M[m_{\text{wd}}])$ data needed for evaluating (numerically) the differential luminosity function $n(L)$.

Figure 6 shows examples of theoretical luminosity functions resulting from such calculations. Each curve gives the dependence of $n(L)$ on the luminosity for a given assumed age of

the stellar system of interest (the Galactic disk in the present case). The ages considered vary from 8 to 16 Gyr, in steps of 1 Gyr. We point out that, for these relatively large values, the shape of the theoretical luminosity function is not sensitive to the age of the stellar system at the higher luminosities, so it is customary to normalize the model luminosity function to an observational point at these luminosities. In the absence of such an observational datum, we normalized all the luminosity functions shown in Figure 6 at an arbitrary point, $L/L_{\odot} = 10^{-3}$ and $n = 10^{-3.48}$, on the ascending branch. The figure shows that white dwarfs pile up with decreasing luminosity until the less massive, more numerous stars start to drop off in large numbers from the mass spectrum present at a given luminosity because they have not had the time to cool to that luminosity. For the range of ages considered in our example, this downturn occurs around $L/L_{\odot} \sim 10^{-4}$. The maximum in the density of expected white dwarfs is then followed, at still lower luminosity, by a fairly sharp decrease. Unlike the ascending branch of the luminosity function, the shape of the descending branch is quite sensitive to the age of the stellar system, and, hence, it is the descending branch that gives the potential for inferring the ages of various populations of white dwarfs. The descending branch, or low-luminosity tail of the luminosity function, is populated by the more massive, less numerous, and oldest white dwarfs in a given population. Indeed, because of the phenomenon of Debye cooling, the more massive stars among the oldest ones reach down to lower luminosities in a given time than the more representative, average-mass white dwarfs in the population.

An interesting feature of the luminosity functions shown in Figure 6 is the obvious bump or peak structure centered around $L/L_{\odot} \sim 10^{-4}$ and corresponding to an extra pileup of white dwarfs beyond what would be expected from a simple extrapolation of the slope of the ascending branch below $L/L_{\odot} \sim 10^{-3.7}$. From our discussion of Figure 5 above, it is clear that this feature bears the combined signatures of both convective coupling and crystallization. However, the contribution of the latter process to that feature is significantly less than that of the former, because the release of latent heat operates over a relatively wide range of luminosities and, consequently, its effects tend to be averaged out over that luminosity interval. We thus reiterate here our conclusion that convective coupling leaves a stronger imprint on the luminosity function than the release of latent heat. However, crystallization still shows its effects via the low-luminosity tail of the distribution. Indeed, the detection of stars belonging to such a tail in a given complete sample constitutes the best observational proof that crystallized white dwarfs do exist.

To finish with this discussion of the most important properties of representative models of cooling white dwarfs, we return briefly to the question of the effects of changing the core composition on the cooling time. We stated above that, provided all other things are kept the same, pure C core models take longer to reach the very low luminosities of interest for cosmochro-

nology than models with cores constituted of either pure O or more realistic mixtures of C and O. To provide the reader with a more quantitative understanding of this, we show, in Figure 7, the cooling curves of three similar $0.6 M_{\odot}$ DA models that differ *only* in the different chemical composition assumed in the core. Model 3 is our standard pure C core model belonging to our family of 23 template models. In comparison, model 1 has a pure O core, and model 2 has a uniformly mixed C/O core in equal proportions per mass ($X_C = X_O = 0.5$). The evolution of the latter model does not include the sedimentation of the two species upon crystallization. The figure shows the cooling curves in a slightly different format than above and focuses only on the very low luminosity phases of the evolution, which are those of interest for white dwarf cosmochronology in most applications. Most of the regime covered by the figure corresponds to late evolutionary phases when convective coupling has already occurred, the crystallization front is well advanced into the star, and Debye cooling has begun. We can estimate from the figure that the pure C core model takes ~ 2.4 Gyr longer than the pure O core model to cool to a luminosity of $L/L_{\odot} = 10^{-4.5}$. This difference grows to ~ 3.6 Gyr at a luminosity $L/L_{\odot} = 10^{-6}$. The model with a mixed core composition shows, as expected, a cooling time intermediate in value. These differences are quite substantial.

4. ILLUSTRATIVE APPLICATIONS OF WHITE DWARF COSMOCHRONOLOGY

4.1. White Dwarfs in the Solar Neighborhood

Our above discussion of the HR diagram revealed that the cooling time of a white dwarf is a strong function of both its mass and effective temperature. It follows that the best way to estimate the ages of individual stars is to compare theoretical isochrones with observational data points in a mass–effective temperature diagram. Of course, the success of the procedure rests on the availability of reliable estimates of M and T_{eff} . For relatively hot white dwarfs, the surface gravity, $\log g$, is usually determined through line profile fitting techniques, while T_{eff} is measured through the same spectroscopic analyses and/or through photometric methods. Given $\log g$, the mass is next inferred via the mass–radius relation imposed by a given set of evolutionary models. For older, cooler white dwarfs, however, the spectroscopic lines have all but disappeared, so the surface gravity cannot be determined through spectroscopy. In that case, one has to rely on parallax measurements to ultimately infer the mass. This limits the method to nearby stars.

The best source of data that currently exists in this context is the exhaustive and systematic study of local cool and very cool white dwarfs carried out by Bergeron et al. (2001, hereafter BLR), who have singled out objects with reliable parallaxes drawn from the Yale Parallax Catalog and from a proper motion survey in the southern hemisphere. BLR have secured optical *BVRI* and infrared *JHK* photometry for each of 152 individual cool white dwarfs. They next χ^2 -fitted each observed energy

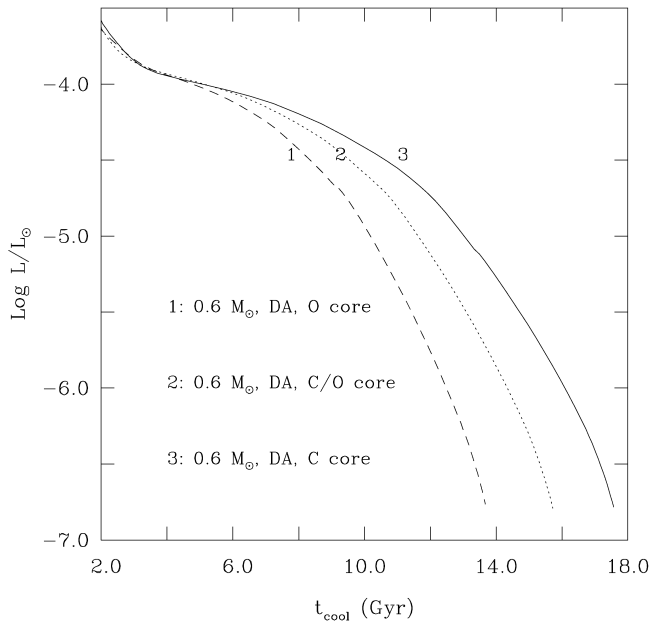


FIG. 7.—Cooling curves for three $0.6 M_{\odot}$ DA white dwarf models differing only in the assumed chemical composition of the core. The pure C core model takes longer to cool down to these low luminosities than its counterparts.

distribution with a theoretical model to obtain a solid angle and the effective temperature. Given the solid angle and the known distance through the parallax, they then determined the radius and, ultimately, the mass through a mass-radius relation.

Figure 8 shows the distribution in the M - T_{eff} diagram of the 135 white dwarfs cooler than $T_{\text{eff}} = 10,000$ K in the BLR parallax sample. In order not to clutter the diagram too much, we plotted only the average error box in the upper right corner. We also superposed two sets of isochrones in the figure. The solid curves correspond to the ages based on the white dwarf cooling phase only (t_{cool}), while the dotted curves correspond to the more realistic values taking into account the time spent on the main sequence by the white dwarf progenitors ($t_{\text{cool}} + t_{\text{ms}}$). We assumed the same IFR and the same main-sequence lifetime law as those used in our calculations of the luminosity functions shown in Figure 6 above. The S-shape of the latter isochrones is readily understandable in terms of the effects of Debye cooling at the top and in terms of the finite lifetimes of the progenitors at the bottom. In particular, the dotted curves illustrate quite well a known result: the fact that single star evolution theory does not allow the formation of white dwarfs less massive than about $\sim 0.45 M_{\odot}$ within a Hubble time. What are then the objects with apparently lower masses than this in Figure 8?

According to BLR, most of these data points correspond to unresolved double degenerate stars that are interpreted as single overluminous objects. At a given effective temperature, this means a larger radius and, therefore, a smaller mass according to the peculiar mass-radius relation that characterizes degen-

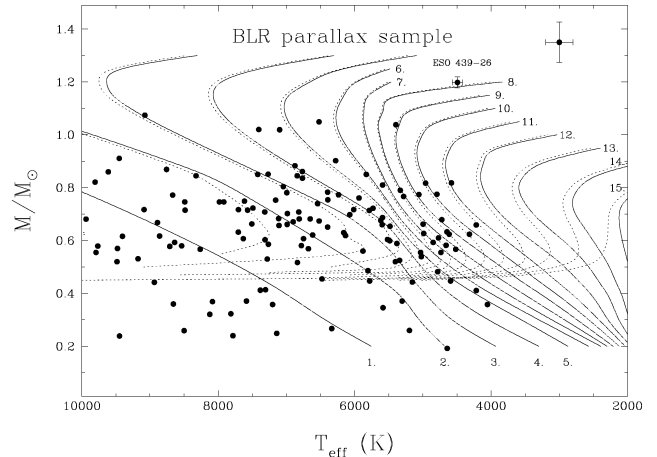


FIG. 8.—Distribution of 135 cool white dwarfs in the M - T_{eff} diagram. These stars are culled from the BLR parallax sample. The average uncertainties on the determinations of the individual values of M and T_{eff} are indicated by the cross in the upper right corner. To compare with theoretical expectations, two sets of isochrones are shown. These are expressed in units of Gyr. The solid curves correspond to the white dwarf cooling phase only, while the dotted curves take into account the lifetimes of the progenitors on the main sequence. The objects with apparent masses below $\sim 0.45 M_{\odot}$ in the figures are either unresolved double degenerates or single stars resulting from common-envelope binary evolution. A comparison of their positions with the isochrones is meaningless in their cases. For the other stars, on the other hand, individual ages can be directly inferred. In particular, the two oldest stars in the sample have ages close to ~ 11 Gyr. This provides an estimate of the age of the Galactic disk.

erate stars. At the same time, some of these objects are believed to be genuine single white dwarfs, but with pure helium cores, the products of binary evolution in a common envelope. In such cases, the pre-white dwarf lifetime on the main sequence is much shorter than that associated with a single star progenitor. Isochrones of varying sophistication for these rare, low-mass, pure He core white dwarfs have been published, for example, by Aparicio & Fontaine (1999), Hansen (1999), Driebe et al. (1999), and others. They are not shown here.

A comparison of the dotted isochrones with the observational points in Figure 8 provides estimates of the ages of a reasonably large number of cool white dwarfs. This is actually the best method available for individual objects. In this context, we singled out ESO 439-26 in the figure (further discussion of it is also presented below). This star is the intrinsically faintest known white dwarf in our neighborhood and, on this basis, has been interpreted by some as the oldest one in our local region of space. As discussed in BLR and as is plainly evident here, ESO 439-26 has an age of ~ 8 Gyr and is clearly not the oldest star in the BLR sample. It is the most massive one, however, and owes its intrinsic faintness to both its low effective temperature *and* small radius. Of greater interest still in the context of white dwarf cosmochronology, Figure 8 reveals that the oldest white dwarfs in the BLR sample are two stars that fall very close to the 11 Gyr isochrone. Because the BLR sample

is representative of the solar neighborhood, this simple comparison in the $M-T_{\text{eff}}$ diagram provides a first estimate of the age of the disk.

We note that a more formal approach to the age of the disk is through luminosity function studies. On this account, as useful as it is for individual stars, the BLR sample is not adequate. Indeed, the sample is eclectic and is not complete in the usual astronomical sense of the term. Instead, two recent independent investigations (based on smaller but *complete* samples) have provided the best determinations of the local cool white dwarf luminosity function currently available. The first study is that of Leggett, Ruiz, & Bergeron (1998), who reconsidered the sample originally surveyed by Liebert et al. (1988), except that the former authors have provided much improved estimates of effective temperatures, bolometric corrections, and absolute magnitudes. It contains 43 objects and constitutes a complete proper motion survey. The second study is that of Knox, Hawkins, & Hambly (1999), who also considered a complete survey, but based on a colorimetric approach. Their sample contains 58 objects.

We first rebinned the luminosity function data of Leggett et al. (1998) in order to compare as closely as possible with the published data of Knox et al. (1999). In the process, we adopted the prescription of Knox et al. (1999) and computed the average luminosity of the stars in a given luminosity bin instead of adopting the usual approach of taking the central luminosity of a bin. This provides a better description of the stars in a bin and allows estimates of the uncertainties in luminosity to be evaluated. We thus obtained four pairs of data points that may be compared directly, as shown in Figure 9. The first remarkable result of this comparison is that, given the usual uncertainties in this business, the data points in common between the two studies agree extremely well. It is appropriate to recall, in this context, that one survey is a proper motion survey and the other is a colorimetric survey. The second noticeable result is that *both* surveys clearly suggest the existence of a bump in the luminosity function, peaking around 10^{-4} solar units in luminosity. Quite interestingly, this bump, or excess of white dwarfs, is naturally expected from theory—at least from our improved cooling models—and corresponds to the delays in cooling associated mostly with the effects of convective coupling.

To show this, we plotted, in Figure 9, theoretical luminosity functions assuming various ages for the white dwarf population, from 8 to 14 Gyr, in steps of 1 Gyr. These curves are a subset of those discussed in Figure 6 above. It is obvious from the figure that the theoretical expectations for the existence of a bump in the luminosity function are well borne out by the observations. This result can be taken as the first direct proof for the existence of convective coupling in white dwarfs. As discussed in a previous section, there is some contribution to this excess in relative white dwarf density coming from the release of latent heat upon crystallization, but this contribution remains relatively small owing to smearing of the effect over

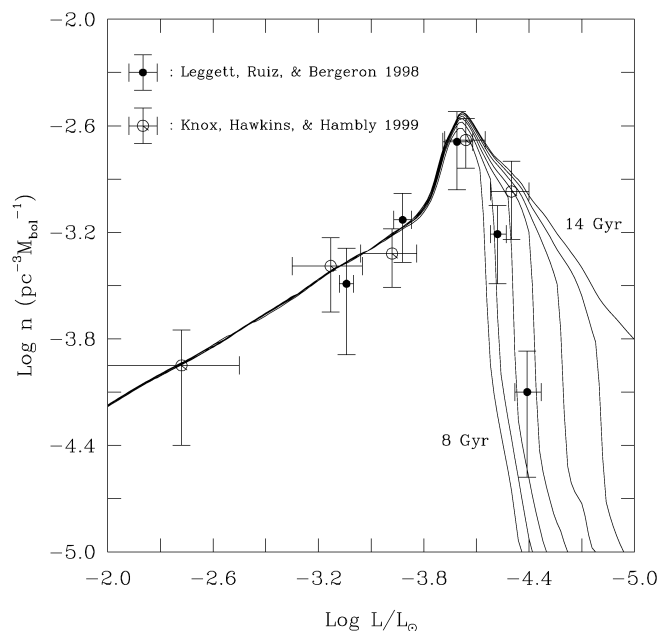


FIG. 9.—Comparison of the observational and theoretical luminosity functions of local white dwarfs and the age of the disk. The data points come from two separate studies, one based on a proper motion survey (Leggett et al. 1998) and the other on a colorimetric survey (Knox et al. 1999). The solid curves are theoretical luminosity functions computed on the basis of our recent cooling models with an assumed pure C core composition. These curves are normalized at a point near $L/L_{\odot} \sim 10^{-3.5}$ on the ascending branch corresponding to the average location of a small cluster of four observational points. Various ages for the white dwarf population in the disk, from 8 to 14 Gyr, are considered.

the mass spectrum. We point out that the existence of this “fine-structure” feature in the luminosity function of local white dwarfs has never been discussed or even mentioned in the past, and its current identification must therefore be seen as a consequence of considerable improvements in the data and in our ability to model cooling white dwarfs.

The most important outcome of the present comparison between observational and theoretical luminosity functions, however, is the determination of the age of the disk. Although the Knox et al. study has a bright bin that happens to fall quite nicely on the ascending branch of the normalized theoretical luminosity functions, the Leggett et al. study is more useful in the present context as it provides a fainter bin that is critical for the actual comparison with the theoretical curves. Figure 9 indicates that the number density of local white dwarfs generally increases with decreasing luminosities until it reaches a maximum, followed by an important dropoff at still lower luminosities.

The simplest explanation for the observed dropoff of the density of white dwarfs at low luminosities, and the one that has been accepted quite generally, is that the first white dwarfs that were formed in the disk and that are now in our neighborhood are still bright enough to be visible. Most of them,

with representative or average masses, have piled up at a luminosity $L/L_{\odot} \sim 10^{-4}$, while the more massive of them, much less numerous, have trickled down through Debye cooling to lower luminosities during the same time and populate the tail at the faint end of the luminosity function.

A comparison of the curves in Figure 9 with the observed points, particularly the coolest bin, suggests an age slightly less than 11 Gyr for the local disk. This is quite consistent with our previous estimate for the age of the oldest white dwarfs in the BLR parallax sample. We recall that these estimates are related to the assumption of a pure C core in our evolutionary models and are likely upper limits to the actual age of the Galactic disk. We also point out that the integration of the luminosity function for an age of 11 Gyr shown in Figure 9 leads to a local density of *single* white dwarfs of 0.0039 pc^{-3} , a value consistent with the original estimate of Liebert et al. (1988).

4.2. White Dwarf Populations in Distant Clusters

To study faint white dwarf populations in distant systems such as open and globular clusters, one often has to deal with what could be called “minimal” or two-band photometry that produces a single color-magnitude diagram (CMD). Cooling theory can be used in conjunction with model atmospheres to compute the evolutionary tracks and plot isochrones in the CMD. To illustrate what can be expected from such a CMD, we first show, in Figure 10, the distribution of the cool white dwarfs in the BLR parallax sample in a standard M_V versus $V-I$ diagram. We also show the evolutionary path followed by a $0.45 M_{\odot}$ DA white dwarf model (*upper dotted curve*) as well as that followed by a $1.2 M_{\odot}$ model (*lower dotted curve*). The $0.45 M_{\odot}$ track provides an envelope, a boundary in the CMD above which single star evolution cannot reach. As explained in a previous section, the data points lying above that boundary in Figure 10 are most likely unresolved double degenerates that appear as single overluminous stars. We finally show in Figure 10 the isochrones (*heavy solid curves*) that take into account the lifetimes of the white dwarf progenitors on the main sequence. As usual, those are expressed in units of Gyr. Similar isochrones have been published by Richer et al. (2000), Chabrier et al. (2000), and Salaris et al. (2000).

We note that the photometric accuracy of the BLR sample is sufficiently high (typically 3% in both V and I according to BLR) that fairly reliable estimates of the ages of individual stars can again be obtained here through a simple comparison of the observed positions in the CMD with the isochrones. These estimates—based on two-band photometry only—are generally in good agreement with the more accurate assignments that can be made from a $M-T_{\text{eff}}$ diagram as demonstrated above. In particular, the two oldest stars that we identified in Figure 8 fall again very close to the 11 Gyr isochrone in the M_V versus $V-I$ diagram. However, at the faint end, the bending of the cooling tracks complicates matters. For example, the intrinsically faintest white dwarf in the BLR sample, ESO 439-26 with

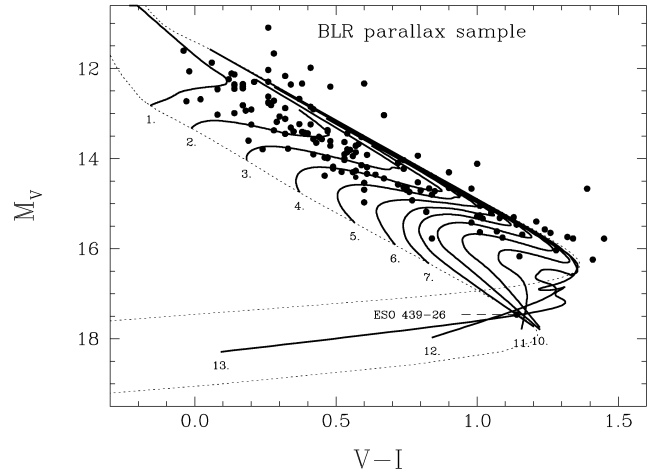


FIG. 10.—Distribution in the M_V vs. $V-I$ color-magnitude diagram of the cool white dwarfs in the BLR parallax sample (*small filled circles*). Evolutionary tracks are shown for two of our reference DA models; one with a mass of $0.45 M_{\odot}$ (*upper dotted curve*) and the other with a mass of $1.2 M_{\odot}$ (*lower dotted curve*). Isochrones, expressed in units of Gyr, are illustrated by the heavy solid curves. These isochrones take into account the lifetimes of the progenitors on the main sequence.

$M_V = 17.47$ and $V-I = 1.14$, can be identified, *on the basis of this CMD alone*, either as a relatively young (~ 8 Gyr) massive ($\sim 1.2 M_{\odot}$) star—which it is!—or as a more typical, less massive object with an age anywhere above that value and up to 13 Gyr. This example underlines the real difficulty of assigning ages to DA white dwarfs in this particular region of the M_V versus $V-I$ diagram where the cooling tracks bend and, consequently, the isochrones loop, twist, and overlap. The complicated structure of the isochrones for $M_V > 16.5$ makes it difficult to play the game of cosmochronology for cosmologically interesting ages on the sole basis of V and I photometry. This should be kept in mind in the planning of future observations of faint white dwarfs in distant and very old systems.

Hansen (1998) was the first one to draw attention to the fact that cooling DA white dwarfs turn to the blue again (at least as measured by the $V-I$ index) when they reach the very late phases of their evolution. The bending of the cooling tracks in the previous M_V versus $V-I$ diagram is indeed a characteristic of the hydrogen-atmosphere stars and is due to the formation of H_2 molecules in their atmospheres when $T_{\text{eff}} \lesssim 4000$ K. These molecules show an opacity that is particularly strong in the near-infrared, thus forcing the flux to escape at other wavelengths. As an illustration of this phenomenon, we present, in Figure 11, the emergent flux (*solid curves*) of an evolving representative $0.6 M_{\odot}$ DA white dwarf model at four effective temperatures (from top to bottom, 13,500, 7500, 4500, and 1500 K) and as a function of wavelength in the optical and near-infrared regions of the spectrum. For comparison purposes, the corresponding blackbody distributions are illustrated by the dotted curves. As seen through the V and I bandpasses

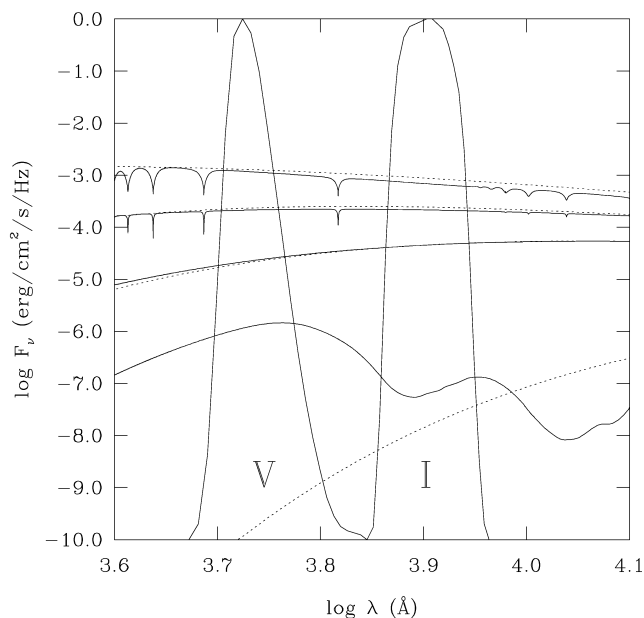


FIG. 11.—The evolution of the emergent flux of a cooling $0.6 M_{\odot}$ DA white dwarf in the optical and near-infrared domains is illustrated in terms of four “snapshots” taken at $T_{\text{eff}} = 13,500, 7500, 4500,$ and 1500 K (solid curves, from top to bottom). The corresponding blackbody distributions are shown by the dotted curves. The normalized transmission curves for the V and I bandpasses are also superposed.

(whose normalized transmission curves are also shown), the star gets progressively redder with decreasing effective temperature until H_2 molecules form in abundance in its atmosphere. For example, at $T_{\text{eff}} = 1500$ K, the flux is distinctly non-Planckian and is considerably larger in the V than in the I filter, so the star has become “blue” again on the basis of the $V-I$ color index.

It should be understood that, contrary to the case of the nearby stars studied by BLR, the photometric scatter of white dwarfs in CMDs derived from observations of distant stellar clusters is generally quite large. This implies that only qualitative results can be obtained from the direct comparison of isochrones with observational points in such diagrams. Figure 12 provides an interesting example of such a confrontation between white dwarf isochrones in a M_V versus $V-I$ diagram and actual data from a star cluster.² The data points were drawn from the Canada-France-Hawaii Telescope (CFHT) study of Richer et al. (1998) of the old open cluster M67. This system has a well-known distance modulus of 9.59. As we just mentioned, it is pointless to try assigning ages to individual objects here because the white dwarfs in M67 are apparently quite faint and, therefore, the photometric scatter is considerable. Nevertheless, the observations reported in Figure 12 are remarkable in that they bear clearly the signature of the finite age of the

² We note, in this context, that a valuable compilation of white dwarfs in open and globular clusters has been presented recently by von Hippel (1998).

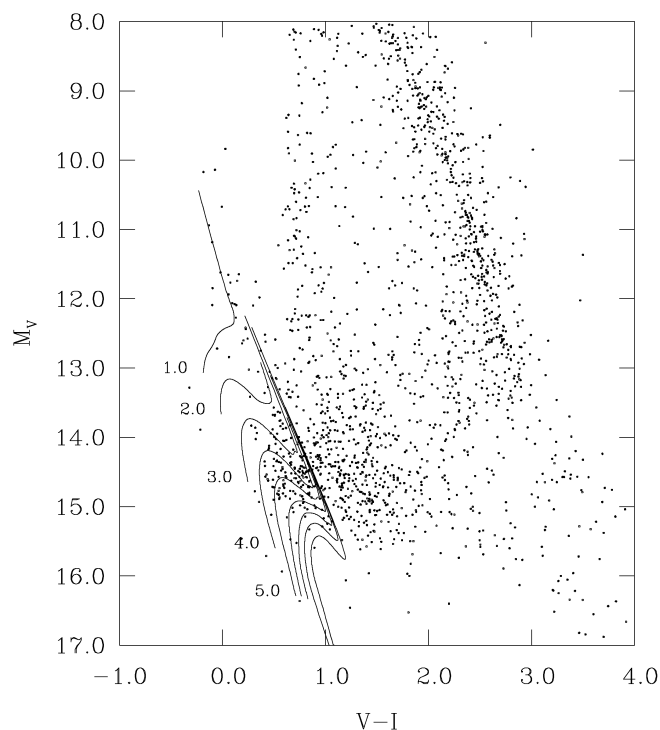


FIG. 12.—Lower part of the color-magnitude diagram (M_V vs. $V-I$) of the old open cluster M67 obtained by Richer et al. (1998) at the CFHT. White dwarf isochrones from 1 to 9 Gyr in steps of 1 Gyr are also superposed (although only the five youngest ones are labeled in order not to clutter the diagram). These isochrones take into account the lifetimes of the progenitors on the main sequence.

white dwarf population in M67. Indeed, it is easy to see in the figure that the white dwarfs show a maximum in density near $M_V \sim 14.6$ and that this maximum is followed, at lower luminosities, by a gradual decrease. This is the expected pileup of white dwarfs at the luminosity characteristic of the age of M67 (the equivalent of the maxima in the luminosity functions shown in Fig. 6). If, contrary to the present case, the sensitivity of the observations is not sufficient to reveal this pileup of white dwarfs in a given cluster, then white dwarf cosmochronology can be used only to provide lower limits to the age of that system.

To exploit properly the information contained in Figure 12, it is necessary to go through detailed stellar counts and statistics and, ultimately, construct an observational luminosity function. This exacting exercise was carried out by Richer et al. (1998), who provided a useful white dwarf luminosity function for M67. We used directly their data, but, in this particular example of application of white dwarf cosmochronology to a star cluster, we regrouped the data into wider luminosity bins in order to improve on the statistics (88 stars distributed in four bins). The resulting observational luminosity function for M67 is presented in Figure 13. The four data points are to be compared with the solid curves which correspond to expected (normal-

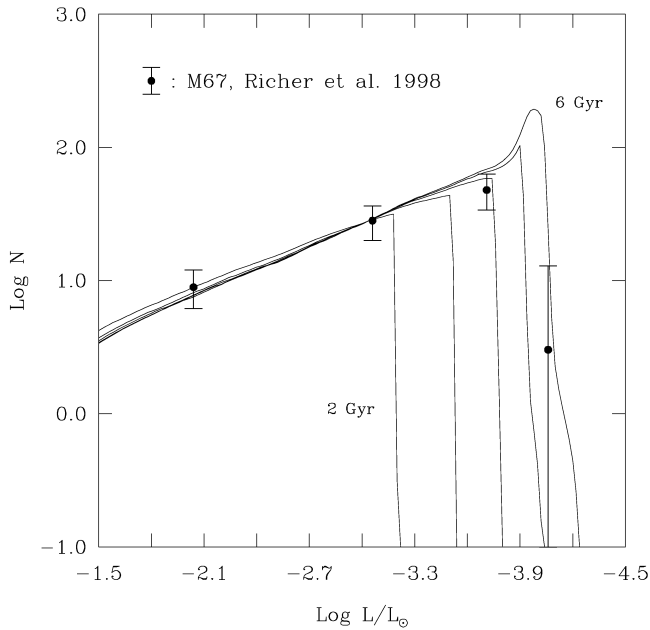


FIG. 13.—Comparison of the observational and theoretical white dwarf luminosity functions for the old open cluster M67. The data points were rebinned from the original data of Richer et al. (1998). The solid curves are theoretical cluster luminosity functions computed on the basis of our template cooling models with an assumed pure C core composition. The curves are normalized to the second observed bin. Various ages for the white dwarf population in M67, from 2 to 6 Gyr in steps of 1 Gyr, are considered.

ized) luminosity functions for various assumed ages for the white dwarf population, from 2 to 6 Gyr in steps of 1 Gyr. These curves match very well the three observational points on the ascending branch, and the observed dropoff in the last bin can be used, as in the case of the disk (Fig. 9 above), to estimate an age for the white dwarf population in M67. Here, the figure suggests an age slightly less than 6 Gyr.

As in the case of the Galactic disk discussed in the previous section, this latest result has to be qualified because it is based on the assumption of pure C core white dwarfs. More realistic C/O core models would lead to a younger age for M67. Unfortunately, among other factors, our partial knowledge of the exact distributions of C and O in the cores of newborn white dwarfs currently limits our ability to pin down the cooling times of these more realistic models (see Salaris et al. 1997 and our discussion above). This implies that the best that we could hope for at the moment from white dwarf cosmochronology is a *continuum* of possible values for the age of M67. Only detailed computations (not yet available) would reveal the extent of this spread of the values, but those would have to be less than 6 Gyr, of course. However, we note that if the age of M67 were to be known with great accuracy from an independent method (such as the turnoff point method, perhaps), then the problem could be turned around and one could adjust the core composition of the white dwarf models until the white dwarf

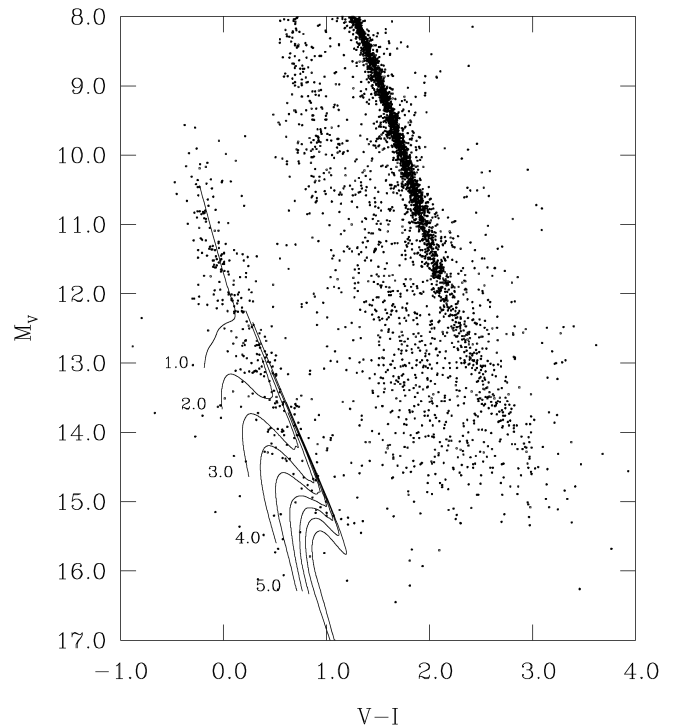


FIG. 14.—Similar to Fig. 12, but for the globular cluster M4. The data were gathered by Richer et al. (1997) with the *Hubble Space Telescope*.

age of M67 would match the turnoff age (say). This would be a wonderful result; the first determination of the mean core composition of white dwarfs in a given homogeneous population. Given, once again, that the exact proportions of C and O in the cores of white dwarfs are still unknown (because of existing uncertainties in the rates of He thermonuclear burning), such a result could shed much needed light on this gray zone of thermonuclear astrophysics.

A second example of the potential of white dwarf cosmochronology as applied to stellar clusters is provided in Figure 14. It shows the lower part of the M_V versus $V-I$ CMD of the globular cluster M4 published by Richer et al. (1997). The data were obtained from *HST* observations, with a limiting apparent magnitude of $V \sim 28$. This system is more distant (its distance modulus is 12.51) and more difficult to analyze than the open cluster M67. Still, the bright part of the white dwarf sequence in M4 is neatly revealed by these particular observations. The oldest white dwarfs in the system are, however, still beyond the sensitivity limit of this CMD. Indeed, we do not see the expected pileup of white dwarfs along the cooling sequence, the maximum in star density that bears the imprint of the age of the system. All we can say on the basis of a comparison of the data points with the isochrones superposed in Figure 14 is that M4 is at least 9 Gyr old or so. Of course, this is not a terribly exciting or constraining result since M4 is known to be much older than that through other methods. Nevertheless,

the path to the future is clear, and it is hoped that a deeper CMD will be obtained for that object in the near future. We have much to learn about a confrontation of white dwarf cosmochronology and more standard well-established techniques for dating stellar clusters. For a recent example of this, see the work of von Hippel & Gilmore (2000).

4.3. White Dwarfs in the Halo

In the last few years, there has been mounting evidence in favor of the presence of a very old white dwarf population in the Galactic halo. In the context of white dwarf cosmochronology, this development is particularly exciting because such a population could be used, in principle, to obtain an independent estimate of the age of the halo. In addition, these old white dwarfs could contribute significantly—perhaps even in a dominant way—to baryonic dark matter in our galaxy and, by extension, in other galaxies as well.

The first piece of evidence is the documented presence of fast movers in our neighborhood, white dwarfs that have very large space velocities and that are best interpreted as interlopers from the halo. In a recent paper, Ibata et al. (2000) have reported the discovery of two cool high proper motion white dwarfs in the solar neighborhood, which they identify as members of an ancient white dwarf population in the Galactic halo. Our model atmosphere fits to the available optical photometry published in Ibata et al. (2000) show that the observed energy distribution of the first object, a star named F351-50, is consistent with that of a very cool DA white dwarf with $T_{\text{eff}} \sim 2870$ K (assuming $\log g = 8$), making it an excellent candidate for membership in that ancient halo population. Unfortunately, the energy distribution of such a cool white dwarf is not sensitive to $\log g$, so the mass cannot be inferred. A reliable parallax measurement for F351-50 is thus urgently needed to estimate its mass and, ultimately, its age with the help of a M - T_{eff} diagram.

The second star found by Ibata et al. (2000), F821-07, appears to be the accidental rediscovery of the large proper motion object WD 2316-064 (LHS 542) originally discussed by Liebert et al. (1989). In their earlier proper motion survey, these latter authors have identified five possible halo candidates, nearby white dwarfs with tangential velocities larger than 250 km s^{-1} , and WD 2316-064 is one of them. It turns out that a reliable parallax measurement is available for WD 2316-064 (placing it at a distance of 31 ± 3 pc from the Sun), and that its complete energy distribution (*BVRJHK*) has been studied and analyzed by Leggett et al. (1998) and, more recently, by BLR (see their Fig. 9). BLR found that this star is a helium-atmosphere white dwarf with $T_{\text{eff}} = 4720 \pm 50$ K and $M = 0.68 \pm 0.11 M_{\odot}$. Assuming that it has evolved as a DA star despite its current helium-dominated atmosphere, this implies that WD 2316-064 has an age of ~ 9.5 Gyr on the basis of its position in the M - T_{eff} diagram shown in Figure 8. This is significantly younger than our estimate above of ~ 11 Gyr for the age of the disk and, therefore, makes it unlikely—although

the possibility cannot be totally ruled out—that WD 2316-064 is a member of an *ancient* white dwarf population in the halo. We point out that the star would be even younger than 9.5 Gyr if it has evolved as a non-DA star (see below).

We searched for other possible candidates by reviewing critically the original sample of Liebert et al. (1989) in the light of the results of Leggett et al. (1998) which provide much improved estimates of the stellar parameters for these stars. We find that three of the five objects in that sample (WD 0145-174, WD 1042+593, and WD 1756+827) are most certainly too hot (7750 K, 8340 K, and 7275 K, respectively) to belong to a very old population. The coolest star in the Liebert et al. (1989) sample is WD 2316-064, which we discussed in the previous paragraph. The second coolest one is a DA star, WD 1022+009, which has an estimated value of $T_{\text{eff}} \approx 5350$ K according to Leggett et al. (1998). While this relatively large value of T_{eff} makes it an unlikely candidate, WD 1022+009 *could* still belong to an ancient halo white dwarf population, depending on its mass. For example, Figure 8 reveals that an age larger than 9 Gyr, comparable to that found above for WD 2316-064, is inferred if WD 1022+009 has a mass in the range 0.90 – $1.05 M_{\odot}$. Likewise, almost any value of the age could be accommodated if, by accident, the mass of the star were to fall in a rather restricted mass range on the low side of the mass distribution, i.e., in the interval $0.45 \lesssim M/M_{\odot} \lesssim 0.5$. Indeed, as can be seen in Figure 8, the late (*dotted*) isochrones converge together in this mass range for ~ 5000 K white dwarfs. As in the case of F351-50 above, a good parallax determination is absolutely needed here.

Altogether, we consider it only a remote possibility that WD 2316-064 and/or WD 1022+009 truly belong to a very old population of white dwarfs inhabiting the halo, even though they show large tangential velocities. If one were to insist on that interpretation, however, one could argue that those objects are the younger remnants of stars that were formed in an initial burst of star formation in the halo, a burst that lasted some finite period of time (as opposed to an unlikely pure delta function). On this basis, and taking advantage of the fact that the Liebert et al. (1989) sample is a *complete* one, we used the $1/V_{\text{max}}$ data as well as the stellar parameters of Leggett et al. (1998) to derive a provisional luminosity function for halo white dwarfs. In this exercise, we lumped together WD 2316-064 and WD 1022+009 in a single luminosity bin and obtained $n(L) \approx 10^{-5.39} \text{ pc}^{-3} M_{\text{bol}}^{-1}$ at $L \approx 10^{-4.09}$. This single-point luminosity function updates and replaces the halo luminosity function originally presented by Liebert et al. (1989). We return to the possible cosmochronological exploitation of this data point in a paragraph below.

A more secure and convincing case in the present context is that of WD 0346+246, another nearby cool white dwarf with clear halo kinematic characteristics. This object has been studied by a British group who has presented a very important series of papers on WD 0346+246 (Hambly, Smartt, & Hodgkin 1997; Hambly et al. 1999; Hodgkin et al. 2000). Quite interestingly, these authors have secured a parallax for that star

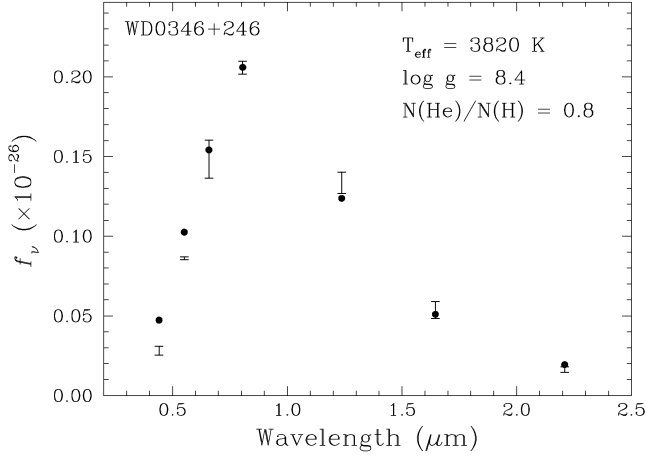


FIG. 15.—Model fit (*small filled circles*) to the observed (*error bars*) energy distribution (*BVRJHK*) of the nearby high proper motion white dwarf WD 0346+246. The *B* and *V* points have not been used in the fit because the models systematically overestimate the flux in these bandpasses. It is believed that an unknown opacity source is responsible for this documented behavior in models of very cool DA white dwarfs.

(placing it at a distance of 28 ± 4 pc from the Sun) and have also published multiband photometry extending into the infrared domain. This has allowed us to use the same tools developed in BLR to analyze the energy distribution of the star. Figure 15 shows the observed energy distribution (*BVRJHK*) of WD 0346+246 as well as our preliminary fit to the data. The fit shows that the *B* and *V* magnitudes are not well reproduced (in fact, they have not been used in the χ^2 exercise, but this is a known phenomenon for very cool DA white dwarfs, likely related to a missing source of pseudocontinuum opacity originating from the hydrogen Lyman edge, as discussed in more detail in Bergeron et al. (1997). Our fit, in conjunction with the known distance and the mass-radius relation imposed by our evolutionary models, suggests that WD 0346+246 has an effective temperature of 3820 ± 50 K, a radius of $0.0099 \pm 0.0014 R_{\odot}$, a mass of $0.80 \pm 0.13 M_{\odot}$, a (logarithmic) surface gravity of 8.35 ± 0.20 , and a luminosity $\log L/L_{\odot} = -4.73 \pm 0.12$. We also find that the atmosphere of WD 0346+246 shows a rare H/He mixed composition with $N(\text{He})/N(\text{H}) \approx 0.79$. On the basis of the pure C core models used in this paper, these values of T_{eff} and M lead to an age of ~ 12.7 Gyr for WD 0346+246 (see Fig. 8), significantly larger than the estimated age of ~ 11 Gyr for the local disk, as derived above. This makes WD 0346+246 a very likely member of the putative family of local white dwarfs belonging to an old halo population. The other candidates are currently F351-50 and, possibly, WD 2316-064 and WD 1022+009 as discussed above.

The second piece of evidence in favor of an old population of white dwarfs in the Galactic halo is more indirect in nature and comes from the MACHO microlensing experiment. We reproduce here a key paragraph taken from one paper published

less than a year ago: “The most straightforward interpretation of the results is that MACHOs make up between 20% and 100% of the dark matter in the halo, and that these objects weigh about $0.5 M_{\odot}$. Objects of substellar mass do not comprise much of the dark matter” (Alcock et al. 1999). Cool white dwarfs are, of course, the most likely candidates for subluminescent objects that “weight” $\sim 0.5 M_{\odot}$. There are problems with this interpretation, mostly related to the appropriate and unknown IMF to be used for the halo, but Chabrier (1999) has shown convincingly how these problems can be worked around. As an illustrative example of this, we computed model luminosity functions for halo white dwarfs assuming that these stars account for a substantial fraction of the dark halo mass. Specifically, to follow up on Chabrier (1999), we considered that 40% (or $0.0078 \times 0.4 = 0.0031 M_{\odot} \text{ pc}^{-3}$) of the dark halo mass density is in the form of cooled off DA white dwarfs. To avoid the problems associated with the formation of too many supernovae in a young halo as well as too many red dwarfs, it is necessary to adopt a bimodal Larson-type IMF (Larson 1986). In this, we follow Chabrier (1999) and use the following IMF,

$$\phi(M) = Ce^{-(2.5/M)^3} M^{-5}, \quad (6)$$

where C is a normalization constant obtained from the condition,

$$\int_{M_l}^{M_u} \phi(M) m_{\text{wd}}(M) dM = 0.0031 M_{\odot} \text{ pc}^{-3}, \quad (7)$$

where $m_{\text{wd}}(M)$ is our usual IFR, $m_{\text{wd}} = 0.4e^{0.125M}$, and the limits of integration are also as above. These limits are somewhat immaterial because the IMF is strongly peaked at the value of the progenitor mass $M^{\text{peak}} = 2.107 M_{\odot}$. This corresponds to a white dwarf mass at the peak of the mass spectrum $m_{\text{wd}}^{\text{peak}} = 0.521 M_{\odot}$, which is close to the suggested value of $\sim 0.5 M_{\odot}$ from the MACHO experiment. If we adopt this value as the average mass of the white dwarf population in the halo, the white dwarf density is $0.0031/0.521 = 0.006 \text{ pc}^{-3}$. Finally, we model the SFR in terms of an initial burst of star formation, followed by an exponential decay with a time constant of 0.5 Gyr,

$$\psi \propto e^{-(t_{\text{halo}} - t_{\text{cool}} - t_{\text{ms}})/(0.5)}, \quad (8)$$

where the characteristic times, t_{halo} , t_{cool} , and t_{ms} , are expressed in units of Gyr. As in the case of the disk, we evaluated the luminosity functions by integrating numerically equation (4) above. The same main-sequence lifetime law was used, $t_{\text{ms}} = 10M^{-2.5}$ Gyr.

Figure 16 shows the model luminosity functions assuming values of the age of the halo, t_{halo} , of 12, 14, and 16 Gyr. Note that these functions are self-normalized; the area under each curve (times 2.5) gives back the assumed white dwarf density in the halo, i.e., 0.006 pc^{-3} . The figure confirms the general

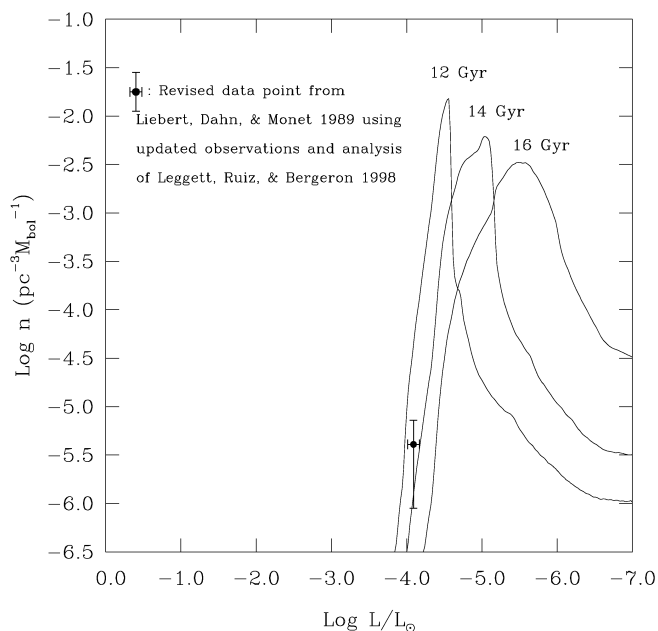


Fig. 16.—Comparison of the observational and theoretical luminosity functions of halo white dwarfs and the age of the halo. The data point comes from our revision of the data of Liebert et al. (1989) in the light of the updated observations and analysis of Leggett et al. (1998). The solid curves are model luminosity functions computed on the basis of our reference cooling DA models with an assumed pure C core composition. Each curve is self-normalized in that its integral corresponds to an assumed halo white dwarf density of 0.006 pc^{-3} . Three values for the age of the white dwarf population in the halo (12, 14, and 16 Gyr) are considered.

expectation that the stars that may have been formed in an initial burst of stellar formation in the newborn halo would have piled up by now as very low luminosity white dwarfs. Quite interestingly, if we compare our single-point luminosity function derived above for local halo white dwarfs with the theoretical curves, we find an estimate of ~ 13 Gyr for the age of the halo, significantly larger than the age of ~ 11 Gyr inferred previously for the disk. This estimate of the age of the halo also appears, within the uncertainties, quite consistent with the age of ~ 12.7 Gyr found above for WD 0346+246. Some caution should certainly be exercised here because the curves shown in Figure 16 have very large slopes on their high-luminosity side, and they can be shifted in luminosity by picking different IMFs. We point out in this respect that, within the framework of the IMF model proposed by Chabrier (1999) for the halo, our choice of parameters entering $\phi(M)$ above has not been totally arbitrary. Instead, we have sought a choice that would lead to a maximum mass in the white dwarf mass spectrum close to the suggested MACHO value of $\sim 0.5 M_{\odot}$. With due caution then, and after all, it is perhaps not too far-fetched to imagine that WD 2316-064 and WD 1022+009 are the younger members of an ancient (~ 13 Gyr) white dwarf population belonging to the Galactic halo!

The third development is due to Hansen (1998), who published a key paper pointing out that some of the so-called blue un-

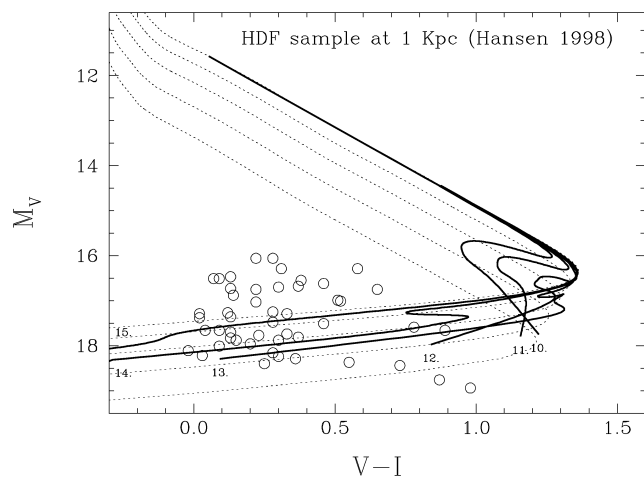


Fig. 17.—Distribution of the so-called blue unidentified HDF objects (*open circles*) in the M_V vs. $V-I$ color-magnitude diagram assuming that they are all located at a typical distance of 1 kpc. To compare with, evolutionary tracks (*dotted curves*) are plotted for models with $M = 0.45, 0.6, 0.8, 1.0,$ and $1.2 M_{\odot}$ (from top to bottom), as well as late isochrones (*heavy solid curves*) for ages from 10 to 15 Gyr in steps of 1 Gyr. These isochrones take into account the lifetimes of the progenitors on the main sequence.

identified objects in the Hubble Deep Field (HDF) could be associated with very old DA white dwarfs in the halo (see also Chabrier et al. 1996). The presence of such objects there would be in line with the results of the MACHO experiment. The nature and distances to these very faint objects ($V \sim 26-29$) are not known, but, following Hansen, if we place them at a typical distance of 1 kpc characteristic of the local halo, we find that many of them fall onto the cool “blue” extension of our cooling curves as shown in Figure 17. These positions correspond to very cool DA white dwarfs with $T_{\text{eff}} \sim 2000-3000$ K. As explained above, it is the occurrence of molecular H_2 formation in the atmospheres of very cool DA white dwarfs that is responsible for the bending of the cooling tracks in the M_V versus $V-I$ diagram. Helium-atmosphere white dwarfs do not show this behavior (see, e.g., Fig. 5 in BLR), and they get monotonously redder as cooling proceeds in that diagram. Consequently, if the blue unidentified objects in the HDF sample are to be associated with degenerate stars, those would have to be hydrogen-atmosphere white dwarfs. We note, however, that only a few of these objects could be genuine white dwarfs; otherwise the total inferred mass of the halo in the form of such very cool white dwarfs would be far too high. On the basis of a comparison of the positions of the HDF objects with the isochrones in Figure 17, ages anywhere from 12 to 15 Gyr can be inferred.

To follow up on Hansen’s suggestion, it was necessary to demonstrate that at least some of the blue unidentified objects in the HDF are truly halo stars as opposed to extragalactic objects, namely, they should show small, but measurable, proper motions. Ibata et al. (1999) rose up to the challenge, and using second-epoch HDF exposures, they reported the probable discovery of detectable proper motions in up to five “blue unidentified objects”

in the HDF. While this exciting discovery awaits confirmation through third-epoch observations (currently under way), corroborating evidence that some of the faint blue point-source objects detected in *both* the HDF North and South could be ancient halo white dwarfs at distances closer than ~ 2 kpc from the Sun has been put forward by Méndez & Minniti (2000). In the meantime, our analysis of the available photometry of the extremely faint objects ($I \sim 28$) uncovered by Ibata et al. (1999) confirms their suggestion that two of these “high” proper motion objects have energy distributions compatible with those of very cool DA white dwarfs while the other three objects do not. This is perfectly compatible with the expectations of Chabrier et al. (1996) and Hansen (1998), the latter estimating that two or three cool halo white dwarfs should be found in the narrow HDF. We find that, if we assume a typical value of $\log g = 8$ for both stars, 4-492 has $T_{\text{eff}} \approx 2500$ K and is located at ~ 2.1 kpc, while 4-551 has $T_{\text{eff}} \approx 2210$ K and is located at a distance of ~ 1.2 kpc. The masses of these stars cannot be estimated on the basis of the observations currently available, so their ages cannot be inferred at the moment. Nevertheless, the case for 4-492 and 4-551 as genuine halo white dwarfs appears quite strong.

We summarize this discussion with the help of Figure 18, which shows the cool side of the M - T_{eff} diagram previously discussed in Figure 8. The solid curves are the isochrones that take into account the lifetimes of the progenitors on the main sequence. We plotted the position of WD 0346+246 along with the formal 1σ errors derived from our fit to the observed multiband photometric data. We also plotted the band of possible effective temperatures for each of the presumed \sim kilo-parsec stars 4-551 and 4-992 as well as for the nearby star F351-50. Again, because we do not know the masses of these three objects, we have to assume plausible values of $\log g$ to estimate T_{eff} , and this leads to bands of effective temperatures which are open-ended at both the top and the bottom. Unfortunately, this implies that a fairly wide range of ages can be accommodated for each of these cool stars. If we insist on the very provisional value of the age of the halo derived above, ~ 13 Gyr, a value consistent with the position of WD 0346+246 in the figure, then 4-551, 4-992, and F351-50 would all have to be rather massive white dwarfs, with $M \gtrsim 0.95 M_{\odot}$, in order not to be older(!) than the halo itself. We cannot exclude that these objects are indeed relatively massive, but, at first sight, it does seem odd that the three apparently coolest white dwarfs that we know *all* need to be so. Perhaps the IMF appropriate for this putative population of ancient halo stars did favor relatively massive main-sequence progenitors and, consequently, relatively massive white dwarf remnants. In contrast, if we assume that the masses of our three very cool stars are closer to the more typical value for halo white dwarfs suggested by the MACHO experiment, $M \approx 0.5 M_{\odot}$ (although the uncertainties on this value, not quoted in Alcock et al. 1999, must be fairly large), then ages upward of 15 Gyr are obtained. In such a case, a halo older than the disk by some 4 Gyr would need to be proposed. Given a natural spread in the ages

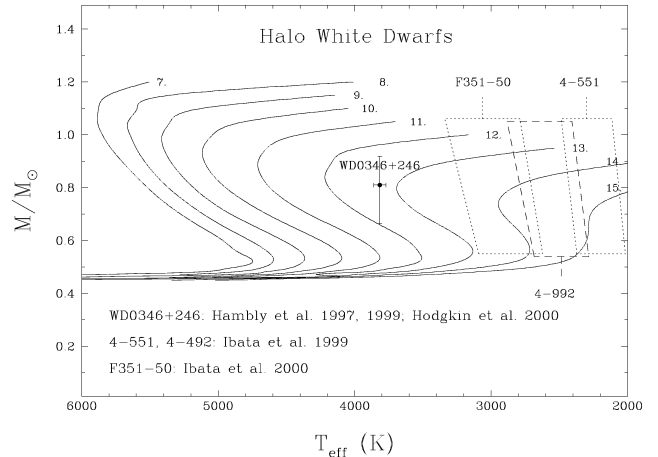


FIG. 18.—Mass-effective temperature diagram for the candidate halo white dwarfs. A secure position is available for WD 0346+246, but in the cases of F351-50, 4-992, and 4-551, the masses are not known. Only bands of possible values of T_{eff} (for assumed values of $\log g$) are inferred from the available observations. These bands are open-ended at both ends. The solid curves show nine isochrones from 7 to 15 Gyr, in steps of 1 Gyr.

of the individual remnants related to the SFR in the halo, WD 0346+246 as well as F351-50, 4-992, and 4-551 could all belong to that ancient population of white dwarfs in the Galactic halo.

5. CURRENT LIMITATIONS OF THE METHOD

The applications of white dwarf cosmochronology discussed in the previous section were meant as illustrative examples of the method. As emphasized several times in the text, our deliberate choice of a pure C core for our evolutionary models is at odds with the expected mixed and inhomogeneous C/O core composition in real white dwarfs. All other things being the same, the ages we derived in our examples are upper limits, and this should be kept in mind. On the other hand, the apparent age *difference* that we found between the disk and the halo is much less sensitive to the assumed core composition. Nevertheless, the estimates of the ages we obtained here need to be revised in the light of models incorporating more realistic core compositions.

In current calculations, the core composition of a white dwarf model is still being considered as an unknown parameter that needs to be varied. For typical white dwarfs, extreme limits can be obtained by considering models with pure C cores and models with pure O cores. For example, a lower limit on the age of the Galactic disk of ~ 8.5 Gyr is obtained by repeating the luminosity function exercise presented in § 4.1, but using models with pure O cores, all other things being again the same as before. This is to be contrasted to our previous upper limit of ~ 11 Gyr obtained on the basis of pure C core models. In principle, the actual age of the disk can be pinpointed, within that range, with much improved accuracy if we take at face

value the results of Salaris et al. (1997) which provide more realistic C/O profiles in newborn white dwarfs. In that case, the major remaining source of uncertainty is the rate of the $C^{12}(\alpha, \gamma)O^{16}$ reaction, although other sources such as the handling of convection and other details of pre-white dwarf evolution also play a role.

Envelope layering is a second parameter of importance in the calculations of the cooling times of white dwarfs since it directly affects the problem of the energy transfer in the models. Treated as a free parameter, its effects have been particularly well studied by Wood (1990). For example, that author found that decreasing the fractional mass of the He layer from 10^{-2} to 10^{-3} increases the time needed for a $0.6 M_{\odot}$ model to cool to a luminosity $L/L_{\odot} = 10^{-4.6}$ by a factor of ~ 19 . In the present work, we assumed, as did several other authors, that typical white dwarfs can be represented by DA models with standard “thick” envelopes. Such models feature a core surrounded by a He mantle containing 10^{-2} of the total mass of the star, itself surrounded by an outermost H envelope containing 10^{-4} of the total mass of the star. We know, however, through empirical facts, that at least some of the DA white dwarfs cannot have such chemical stratification and that they undergo spectral transformation to the non-DA state through convective dilution and mixing of relatively thin outer H layers. Furthermore, the available evidence from asteroseismology, although quite sparse, suggests a wide range of possible values, 10^{-10} to 10^{-4} , for the fractional mass of the outer H layer in a handful of pulsating DA (ZZ Ceti) stars. Hence, DA white dwarfs *cannot* all have the “thick” envelope layering that was assumed in our evolutionary calculations, although it is currently believed that a majority do. This question of envelope layering in white dwarfs, last reviewed by Fontaine & Wesemael (1997), continues to cloud our detailed understanding of white dwarf evolution.

It has been recently emphasized by BLR that spectral evolution, through the changes it brings about on the superficial composition of certain white dwarfs, obscures further the problem of determining the ages of cool white dwarfs. This issue is closely related to the question of envelope layering which is clearly quite different in DA and non-DA objects. Because of this difference, the two types of stars do not evolve at the same rates, particularly in the low-luminosity phases when convective coupling has already occurred. Indeed, it is well known that cool DA stars with “thick” hydrogen layers evolve slower than their non-DA counterparts because their hydrogen outer layers are better insulators than the helium envelopes in non-DA objects. An extreme example of this phenomenon is provided by Hansen (1999), who found that a $0.6 M_{\odot}$ DA model takes ~ 2.5 Gyr longer to cool to a luminosity $L/L_{\odot} = 10^{-5}$ than a $0.6 M_{\odot}$ non-DA model. We note, in passing, that this difference would have been much smaller had Hansen (1999) considered the inclusion of even very small admixtures of metals in his *pure* helium-atmosphere non-DA models. This is because of the extreme transparency reached by neutral helium

at very low temperatures, a phenomenon not observed in a pure hydrogen plasma. The effects of varying the metal mass fraction, Z , on the cooling times of non-DA white dwarfs has not yet been studied quantitatively with modern codes (the available results from these codes are based on the assumption that $Z = 0$). This is yet another parameter that needs to be specified in the computations.

The point made by BLR is that because spectral evolution does take place in white dwarfs (see, e.g., Fontaine & Wesemael 1987, 1997; Bergeron et al. 1997; or BLR), at least a fraction of DA stars become non-DA stars and vice versa, and we cannot be absolutely certain that a given white dwarf has cooled as a pure DA model or as a pure non-DA model. For instance, the mixed atmospheric composition inferred for WD 0346+246 suggests caution. If this star has evolved during most of its life in the form of a DA, then the old age derived above is appropriate. On the other hand, if it has evolved as a non-DA, then it could be a much younger object (for the same values of T_{eff} and M) and could possibly not be of relevance for the question of the existence of an ancient population of white dwarfs in the Galactic halo. Likewise, the low effective temperature derived above for F351-50 does not necessarily imply an old age if, again, it too evolved as a non-DA star. In this particular case, and on the basis of the optical photometry of Ibata et al. (2000) alone, we cannot even distinguish between a hydrogen- and helium-atmosphere white dwarf. The observations of the energy distribution of F351-50 should be extended into the infrared range in order to exploit a sensitivity to the atmospheric composition (see BLR). To conclude this on an optimistic note, however, we point out that a majority of white dwarfs apparently *must* evolve as DA stars because of the excellent agreement shown between the observational and theoretical luminosity functions discussed in Figure 9, including the fine structure associated with convective coupling. We recall in this context that the samples of Leggett et al. (1998) and Knox et al. (1999) are mixed bags of DA and non-DA white dwarfs. In comparison, the theoretical luminosity functions are based on DA models and feature a convective coupling structure whose strength and location are characteristic of these models. Finally, we underline the fact that both 4-992 and 4-551, if confirmed as degenerate dwarfs, must have evolved as DA stars and must be quite old; otherwise, they would not belong to the cool “blue” extension of DA cooling curves in the M_V versus $V-I$ diagram of Figure 17.

On the front of the constitutive microphysics, immense progress has been made in the last decade, but not to the point where we could seriously claim that white dwarf cosmochronology has superseded other methods. Not yet. It has nevertheless often been claimed that the evolution of white dwarfs, a “simple” cooling problem, is so well understood that more accurate ages naturally follow from the applications of white dwarf cosmochronology. We currently think otherwise. The fact of the matter is that white dwarf physics is much more complex, and therefore more uncertain, than main-sequence and giant star physics, and one would be hard pressed to dem-

onstrate, for example, that white dwarf cosmochronology presently gives better estimates of the ages of Galactic clusters than the turnoff point method, especially for the older systems. We believe instead that a confrontation between the two methods (and others) will be most fruitful. One of the major strengths of the white dwarf approach is that white dwarf ages are insensitive to the treatment of convection, which is currently the largest source of uncertainty in the determination of the ages of their progenitors. We recall, however, that it is only recently that the debate concerning the impact of C/O sedimentation upon crystallization in cooling models of white dwarfs has been settled. It is only recently that the importance of including detailed model atmospheres in the evolutionary calculations of very cool stars has been appreciated. It is only in the present paper, because we considered the evolution of *full* models, including the atmosphere/envelope, that the importance of convective coupling came through. We caution that white dwarf evolution, supposedly bland and uneventful, may still have some surprises for us!

Finally, it is appropriate to mention here that an old problem with white dwarf physics, and one which is still very much with us, is the lack of reliable low-temperature *and* high-density radiative opacities in the regime where conduction has not yet taken over. This affects the evolution of cool and very cool white dwarfs models. Currently, in all calculations carried out, some kind of extrapolation technique for the radiative opacity in this extreme regime has been used. It is unlikely that these uncertain data lead to drastic effects on the cooling times, but this missing piece of microphysics must be currently considered as the weakest item on the front of the constitutive physics of white dwarfs.

To complete this overview of white dwarf cosmochronology, we must point out that we barely mentioned the exploitation of low-mass, pure He core white dwarfs as cosmochronometers. Those have been used, among other things, to infer ages of millisecond pulsar systems (see, e.g., Hansen & Phinney 1998; Benvenuto & Althaus 1998; and, more recently, Schönberner, Driebe, & Blöcker 2000). In the interest of space, we have not covered this other fascinating aspect of white dwarf physics in this paper; it would clearly deserve a review in its own right.

6. CONCLUSION

White dwarf cosmochronology is still in its infancy, but it already shows its potential as a powerful tool for estimating the ages of the various components of the Galaxy. Models of cooling white dwarfs, particularly the more recent ones extending into the interesting but difficult regime of very low effective temperatures, need to be improved. In particular, we need to understand better the effects of spectral evolution. We computed a preliminary family of template models extending into this regime in order to illustrate some potential applications of the method. These computations were carried out on the assumption that a majority of white dwarfs evolve as thick-layered DA models. Combined with the latest available observations, our results confine the age of the local disk to the 8.5–11 Gyr interval, with the largest source of uncertainties coming from the unknown exact proportions of C and O in the cores of field white dwarfs. We also obtained a very preliminary estimate of the age of the halo based on white dwarf cosmochronology, as first presented here. Our results suggest that the halo may be significantly older than the disk, by 2–4 Gyr, compared to ~11 Gyr for the disk (using the same pure C core models). Finally, we demonstrated that the potential of the method for dating open and globular clusters is immense. In the era of giant 8–10 m ground-based telescopes, we are just beginning.

We wish to thank the following individuals for reading and, in many instances, providing useful suggestions that have improved the presentation of this paper: Gilles Chabrier, Paul Charbonneau, Stéphane Charpinet, Pierre Chayer, Pierre Demarque, Michael De Robertis, Enrique Garcia-Berro, Nigel Hambly, Gretchen Harris, Bill Harris, Brad Hansen, Margarida Hernanz, Jordi Isern, Jim Liebert, René Méndez, Ben Oppenheimer, Harvey Richer, Maria Teresa Ruiz, Maurizio Salaris, Didier Saumon, Hugh Van Horn, and Ted von Hippel. We are also indebted to Harvey Richer for kindly providing us with the CMD data for the clusters M67 and M4. This work was supported in part by the NSREC of Canada and by the Fund FCAR (Québec).

REFERENCES

- Alcock, C., et al. 1999, in ASP Conf. Ser. 165, The Third Stromlo Symposium: The Galactic Halo, ed. B. K. Gibson, T. S. Axelrod, & M. E. Putman (San Francisco: ASP), 362
- Allard, N. F., Koester, D., Feautrier, N., & Spielfiedel, A. 1994, A&AS, 108, 417
- Aparicio, J. M., & Fontaine, G. 1999, in ASP Conf. Ser. 169, Proc. 11th European Workshop on White Dwarfs, ed. J.-E. Solheim & E. G. Meistas (San Francisco: ASP), 390
- Benvenuto, O. G., & Althaus, L. G. 1998, MNRAS, 293, 177
- . 1999, MNRAS, 303, 30
- Bergeron, P., Leggett, S. K., & Ruiz, M. T. 2001, ApJS, 133, 415 (BLR)
- Bergeron, P., Ruiz, M. T., & Leggett, S. K. 1997, ApJS, 108, 339
- Bergeron, P., Saumon, D., & Wesemael, F. 1995a, ApJ, 443, 764
- Bergeron, P., Wesemael, F., & Beauchamp, A. 1995b, PASP, 107, 1047
- Bergeron, P., Wesemael, F., & Fontaine, G. 1991, ApJ, 367, 253
- Böhm, K.-H., Carson, T. R., Fontaine, G., & Van Horn, H. M. 1977, ApJ, 217, 521
- Chabrier, G. 1993, ApJ, 414, 695
- . 1998, in IAU Symp. 189, Fundamental Stellar Properties, ed. T. R. Bedding, A. J. Booth, & J. Davis (Dordrecht: Kluwer), 381
- . 1999, ApJ, 513, L103
- Chabrier, G., Brassard, P., Fontaine, G., & Saumon, D. 2000, ApJ, 543, 216
- Chabrier, G., Segretain, L., & Méra, D. 1996, ApJ, 468, L21

- Cox, A. N., & Stewart, J. N. 1970, *ApJS*, 19, 261
- D'Antona, F., & Mazzitelli, I. 1978, *A&A*, 66, 453
- Driebe, T., Schönberner, D., Blöcker, T., & Herwig, F. 1999, in *ASP Conf. Ser.* 169, *Proc. 11th European Workshop on White Dwarfs*, ed. J.-E. Solheim & E. G. Meistas (San Francisco: ASP), 394
- Eggleton, P. P., Faulkner, J., & Flannery, B. P. 1973, *A&A*, 23, 325
- Fontaine, G. 1973, Ph.D. thesis, Univ. Rochester
- Fontaine, G., Graboske, H. C., Jr., & Van Horn, H. M. 1977, *ApJS*, 35, 293
- Fontaine, G., & Van Horn, H. M. 1976, *ApJS*, 31, 467
- Fontaine, G., & Van Horn, H. M., Böhm, K.-H., & Grenfell, T. C. 1974, *ApJ*, 193, 205
- Fontaine, G., & Wesemael, F. 1987, in *IAU Colloq. 95, The Second Conference on Faint Blue Stars*, ed. A. G. D. Philip, D. S. Hayes, & J. Liebert (Schenectady: L. Davis Press), 319
- . 1997, in *White Dwarfs, Proc. 10th European Workshop on White Dwarfs*, ed. J. Isern, M. Hernanz, & E. Garcia-Berro (Dordrecht: Kluwer), 173
- Fowler, W. A., Caughlan, G. R., & Zimmerman, B. A. 1975, *ARA&A*, 13, 69
- Garcia-Berro, E., Hernanz, M., & Isern, J. 1997, *MNRAS*, 289, 973
- Garcia-Berro, E., Hernanz, M., Mochkovitch, R., & Isern, J. 1988, *A&A*, 193, 141
- Hambly, N. C., Smartt, S. J., & Hodgkin, S. T. 1997, *ApJ*, 489, L157
- Hambly, N. C., Smartt, S. J., Hodgkin, S. T., Jameson, R. F., Kemp, S. N., Rollerston, W. R. J., & Steele, I. A. 1999, *MNRAS*, 309, L33
- Hansen, B. M. S. 1998, *Nature*, 394, 860
- . 1999, *ApJ*, 520, 680
- Hansen, B. M. S., & Phinney, E. S. 1998, *MNRAS*, 294, 557
- Hernanz, M., Garcia-Berro, E., Isern, J., Mochkovitch, R., Segretain, L., & Chabrier, G. 1994, *ApJ*, 434, 652
- Hodgkin, S. T., Oppenheimer, B. R., Hambly, N. C., Jameson, R. F., Smartt, S. J., & Steele, I. A. 2000, *Nature*, 403, 57
- Hubbard, W. B., & Lampe, M. 1969, *ApJS*, 18, 297
- Ibata, R. A., Irwin, M., Bienaymé, O., Scholz, R., & Guibert, J. 2000, *ApJ*, 532, L41
- Ibata, R. A., Richer, H. B., Gilliland, R. L., & Scott, D. 1999, *ApJ*, 524, L95
- Iben, I., Jr., & Laughlin, G. 1989, *ApJ*, 341, 312
- Iglesias, C., & Rogers, F. G. 1996, *ApJ*, 464, 943
- Isern, J., Garcia-Berro, E., Hernanz, M., & Chabrier, G. 2000, *ApJ*, 528, 397
- Isern, J., Mochkovitch, R., Garcia-Berro, E., & Hernanz, M. 1997, *ApJ*, 485, 308
- Itoh, N., Hatashi, H., & Kohyama, Y. 1993, *ApJ*, 418, 405
- Itoh, N., Hayashi, H., Nishikawa, A., & Kohyama, Y. 1996, *ApJS*, 102, 411
- Itoh, N., & Kohyama, Y. 1993, *ApJ*, 404, 268
- Itoh, N., Kohyama, Y., Matsumoto, N., & Seki, M. 1984, *ApJ*, 285, 758
- Itoh, N., Mitake, S., Iyetomi, H., & Ichimaru, S. 1983, *ApJ*, 273, 774
- Knox, R. A., Hawkins, M. R. S., & Hambly, N. C. 1999, *MNRAS*, 306, 736
- Lamb, D. Q. 1974, Ph.D. thesis, Univ. Rochester
- Lamb, D. Q., & Van Horn, H. M. 1975, *ApJ*, 200, 306
- Larson, R. B. 1986, *MNRAS*, 218, 409
- Leggett, S. K., Ruiz, M. T., & Bergeron, P. 1998, *ApJ*, 497, 294
- Lenzuni, P., Chernoff, D. F., & Salpeter, E. E. 1991, *ApJS*, 76, 759
- Liebert, J., Dahn, C. C., & Monet, D. G. 1988, *ApJ*, 332, 891
- . 1989, in *IAU Colloq. 114, White Dwarfs*, ed. G. Wegner (Berlin: Springer), 15
- Mazzitelli, I., & D'Antona, F. 1986a, *ApJ*, 308, 706
- . 1986b, *ApJ*, 311, 762
- . 1987, in *IAU Colloq. 95, The Second Conference on Faint Blue Stars*, ed. A. G. D. Philip, S. Hayes, & J. Liebert (Schenectady: L. Davis Press), 351
- Méndez, R., & Minniti, D. 2000, *ApJ*, 529, 911
- Mestel, L. 1952, *MNRAS*, 112, 583
- Mochkovitch, R. 1983, *A&A*, 122, 212
- Montgomery, M. H., Klumpe, E. W., Winget, D. E., & Wood, M. A. 1999, *ApJ*, 525, 482
- Noh, H. R., & Scalo, J. 1990, *ApJ*, 352, 605
- Paquette, C., Pelletier, C., Fontaine, G., & Michaud, G. 1986, *ApJS*, 61, 177
- Richer, H. B., Falhman, G. G., Rosvick, J., & Ibata, R. A. 1998, *ApJ*, 504, L91
- Richer, H. B., Hansen, B. M. S., Limongi, M., Chieffi, A., Straniero, O., & Falhman, G. G. 2000, *ApJ*, 529, 318
- Richer, H. B., et al. 1997, *ApJ*, 484, 741
- Rogers, F. G., & Iglesias, C. 1992, *ApJS*, 79, 507
- Salaris, M., Dominguez, I., Garcia-Berro, E., Hernanz, M., Isern, J., & Mochkovitch, R. 1997, *ApJ*, 486, 413
- Salaris, M., Garcia-Berro, E., Hernanz, M., Isern, J., & Saumon, D. 2000, *ApJ*, 544, 1036
- Saumon, D., Chabrier, G., & Van Horn, H. M. 1995, *ApJS*, 99, 713
- Saumon, D., & Jacobson, S. B. 1999, *ApJ*, 511, L107
- Schmidt, M. 1959, *ApJ*, 129, 243
- Schönberner, D., Driebe, T., & Blöcker, T. 2000, *A&A*, 356, 929
- Schwarzschild, M. 1958, *Structure and Evolution of the Stars* (Princeton: Princeton Univ. Press)
- Segretain, L., & Chabrier, G. 1993, *A&A*, 271, L13
- Segretain, L., Chabrier, G., Hernanz, M., Garcia-Berro, E., Isern, J., & Mochkovitch, R. 1994, *ApJ*, 434, 641
- Stevenson, D. J. 1980, *J. Phys. Suppl.*, 41, C2-53
- Tassoul, M., Fontaine, G., & Winget, D. E. 1990, *ApJS*, 72, 335
- Van Horn, H. M. 1971, in *IAU Symp. 42, White Dwarfs*, ed. W. J. Luyten (Dordrecht: Reidel), 97
- von Hippel, T. 1998, *AJ*, 115, 1536
- von Hippel, T., & Gilmore, G. 2000, *AJ*, 120, 1384
- Winget, D. E., Hansen, C. J., Liebert, J., Van Horn, H. M., Fontaine, G., Nather, R. E., Kepler, S. O., & Lamb, D. Q. 1987, *ApJ*, 315, L77
- Wood, M. A. 1990, Ph.D. thesis, Univ. Texas at Austin
- . 1992, *ApJ*, 386, 539
- . 1995, in *White Dwarfs, Proc. Ninth European Workshop on White Dwarfs*, ed. D. Koester & K. Werner (Berlin: Springer), 41
- Wood, M. A., & Winget, D. E. 1989, in *IAU Colloq. 114, White Dwarfs*, ed. G. Wegner (Berlin: Springer), 282
- Yuan, J. W. 1989, *A&A*, 224, 108